



Light Water Reactor Sustainability Program

Assessment of Additional Key Indicators of Aging Cables in Nuclear Power Plants – Interim Status for FY2015



May 2015

U.S. Department of Energy

Office of Nuclear Energy

DISCLAIMER

This information was prepared as an account of work sponsored by an agency of the U.S. Government. Neither the U.S. Government nor any agency thereof, nor any of their employees, makes any warranty, expressed or implied, or assumes any legal liability or responsibility for the accuracy, completeness, or usefulness, of any information, apparatus, product, or process disclosed, or represents that its use would not infringe privately owned rights. References herein to any specific commercial product, process, or service by trade name, trade mark, manufacturer, or otherwise, does not necessarily constitute or imply its endorsement, recommendation, or favoring by the U.S. Government or any agency thereof. The views and opinions of authors expressed herein do not necessarily state or reflect those of the U.S. Government or any agency thereof.

M3LW-15OR0404022
PNNL-24309

Assessment of Additional Key Indicators of Aging Cables in Nuclear Power Plants – Interim Status for FY2015

**P Ramuhalli, LS Fifield, M Prowant, G Dib, JR Tedeschi, JD Suter,
AM Jones, MS Good, SW Glass, AF Pardini**

May 2015

**Prepared for the
U.S. Department of Energy
Office of Nuclear Energy**

Light Water Reactor Sustainability Program

**Assessment of Additional Key Indicators of Aging
Cables in Nuclear Power Plants –
Interim Status for FY2015**

**M3LW-15OR0404022
PNNL-24309**

**P Ramuhalli, LS Fifield, M Prowant, G Dib, JR Tedeschi, JD Suter,
AM Jones, MS Good, SW Glass, AF Pardini**

Approved by:



Steve N. Schlahta
Director, Nuclear Science Project Management Office

May 15, 2015

Date

SUMMARY

This interim report presents an update on the research being conducted to identify key indicators of cable insulation and jacketing material aging at operating light water reactor nuclear power plants (NPPs), and devise in-situ measurement techniques that are sensitive to these key indicators. The motivation for this study stems from the need to address open questions related to nondestructive evaluation (NDE) of aging cables for degradation detection and estimation of condition-based remaining service life. These questions arise within the context of a second round of license extension for NPPs in the United States that would extend plant operating licenses to 80 years.

The most important criterion for cable performance in NPPs is the ability of cables to withstand a design-basis accident. Degradation of the cable jacket, electrical insulation, and other cable components is a key issue that is likely to affect the ability of the currently installed cables to operate safely and reliably for another 20 to 40 years beyond the initial operating life. With greater than 1000 km of power, control, instrumentation, and other cables typically found in an NPP, it would be a significant undertaking to replace all of the cables. The development of one or more NDE techniques and supporting models that could assist in determining remaining life expectancy of cables based on their current degradation state would be of significant interest. The ability to nondestructively determine the properties of cable jackets and insulation without disconnecting the cables has been deemed essential for this purpose.

Currently, the gold standard for determining cable insulation degradation (through a measurement of cable elasticity) is the elongation-at-break (EAB) measurement. This is an ex-situ measurement and requires removing a sample of cable insulation for laboratory investigation. The indentation method is generally accepted by industry as a nondestructive measurement of cable elasticity that correlates well with EAB. However, the vast majority of aging management programs in operating NPPs rely on a combination of visual and tactile assessments performed during walkdowns. Where necessary, these assessments may be augmented with NDE measurements such as insulation resistance, and electrical $\tan \delta$ tests. However, visual, tactile, local electrical, and indentation techniques are applicable only to easily accessible cable sections. All other NDE techniques that are currently used are designed to find flaws in the conductor and do not readily provide information useful for determining the health or life expectancy of cable insulation. Indeed, there is no single NDE technique that can satisfy all of the requirements needed for making a life-expectancy determination, but a wide range of methods have been evaluated for use in NPPs as part of a continuous evaluation program.

There occur several physical and chemical property changes in cable insulation as a result of thermal and radiation damage. In principle, these properties may be targets for advanced NDE methods to provide early warning of aging and degradation. Examples of such key indicators include changes in chemical structure, mechanical modulus, and dielectric permittivity. While some of these indicators are the basis of currently used technologies, there is a need to increase the volume of cable that may be inspected with a single measurement, and if possible, to develop techniques for in-situ inspection (i.e., while the cable is in

operation). Progress towards the evaluation of such key indicators and the ability to measure changes in these key indicators is the focus of the present report.

This report is the latest in a series of reports, each documenting studies on a subset of key indicators. Previous reports examined the applicability of dielectric measurements, measurements of elastic moduli, and preliminary measurements of key chemical indicators of aging to assess condition of thermally aged ethylene propylene rubber (EPR) rubber. The present document examines the ability to measure mechanical moduli using stress-wave-based interrogation methods, as well as the feasibility of applying high resolution infrared (IR) reflectance spectroscopy. Supporting laboratory-based measurement methods that provide insights into the changes in material properties with thermal aging are also presented.

In each case, measurement studies were conducted with specimens of aged medium-voltage EPR cable. Accelerated aging studies were conducted at multiple temperatures using the cable system (short segments of cable with the conductor intact). A test-bed was also fabricated to enable in-situ measurement of current and voltage on an aging cable system (conductor and insulation), along with aging of the smaller specimens of the medium-voltage cable. These specimens were used for measurements of key indicators.

Previous studies with EPR indicated that the complex electrical permittivity appeared to show correlation with aging while preliminary studies on acoustic sound speed showed no clear measurable trend (within the error bounds of the measurements). The primary factor impacting the measurements in the previous study was the unknown and variable thickness of the insulating material. In this study, the measurement protocols were modified to overcome this issue, and to use higher precision probes within a laboratory-scale measurement setup. Measurements of acoustic wave speed using this modified setup show a measurable trend with aging, although the results to date are based on a small set of specimens. Further, in-situ measurements using dynamic mechanical analysis indicate that the storage modulus changes with specimen age; this change is a function of the aging conditions and the environment the specimen is in. However, laboratory-scale measurements using higher resolution IR reflectance spectroscopy (albeit over a narrow portion of the IR spectrum) were inconclusive. It is likely that this result is due to unknown surface conditions on the aged specimens.

Additional studies are ongoing to determine the viability of these approaches for other insulating materials (such as cross-linked polyethylene) that are common in NPPs. At the same time, focus is shifting to develop in-situ measurement approaches for key indicators that show promise, and to evaluate such advanced NDE techniques for sensitivity and reliability.

CONTENTS

SUMMARY	v
ACRONYMS	xi
1. INTRODUCTION	1.1
1.1 Background	1.1
1.2 Overall Project Objectives	1.3
1.3 Objectives of this Report.....	1.3
1.4 Report Organization	1.4
2. KEY INDICATORS OF CABLE DEGRADATION.....	2.1
3. EXPERIMENTAL ASSESSMENT OF KEY INDICATORS.....	3.1
3.1 Materials.....	3.1
3.2 Cable Aging Test-bed	3.2
3.3 Measurement of Chemical Changes Using Infrared Spectroscopy.....	3.5
3.4 Measurement Techniques for Mechanical Properties	3.7
3.4.1 Indenter Modulus	3.7
3.4.2 Dynamic Mechanical Analysis	3.7
3.4.3 Ultrasonic Measurements of Sound Speed and Attenuation.....	3.10
3.4.4 Non-Linear Ultrasonic Measurements	3.14
3.5 Measurement Techniques for Electrical Properties	3.15
3.5.1 Tan δ Measurement Technique	3.16
4. RESULTS.....	4.1
4.1 DMA Measurements	4.1
4.2 Infrared Spectroscopy	4.3
4.3 Indenter Measurements	4.4
4.4 Acoustic Measurements	4.6
4.4.1 Conventional Transducer Measurements.....	4.6
4.4.2 Scanning Pinducer Measurements	4.9
4.5 Coaxial Dielectric Probe Measurements.....	4.12
4.6 Discussion	4.14
5. SUMMARY	5.1
6. PATH FORWARD.....	6.1
6.1 Mechanical Measurements.....	6.1
6.1.1 Ultrasonic Testing	6.1
6.1.2 Alternative Measurements	6.1
6.2 Electrical Measurements.....	6.2
7. REFERENCES	7.1

FIGURES

1.1	Overview of Research Tasks for Cable Aging Detection and Remaining Life Assessment	1.2
3.1	Photo of Cable with EPR Insulation for Use in Measurements of Key Indicators	3.1
3.2	Graphic Representation of Measurement Circuit.....	3.2
3.3	Photograph Showing the Cable Aging Test-bed.....	3.3
3.4	LabVIEW Integrated Control Interface	3.4
3.5	Representative Data Recorded by the Control System	3.4
3.6	ECQCL Spectral Output Compared Against EPR Cable Material Pre- and Post-Aging, as Measured with FTIR Transmission	3.6
3.7	Photograph and Schematic of Cable Test Apparatus.....	3.6
3.8	Image of the DMA Instrument with Compression Tip for Shear Modulus and Photograph of Tensile DMA Instrument Setup with Cable Insulation Specimen Illustration of Input/Output Waveforms that Form the Basis for the DMA Measurement.....	3.8
3.9	DMA Data Schematic Illustrating the Available Information Determined by DMA	3.9
3.10	DMA Data for Un-aged Jumper Cable with EPR Insulation.....	3.9
3.11	Storage Modulus of 140°C Thermally Aged EPR.....	3.10
3.12	Ultrasonic Transducer Configuration for Standoff Measurement of Polymer Sample.....	3.12
3.13	Non-Linear Media Affected Signal Compared to Initial Signal	3.14
3.14	One Test Configuration for Measuring B/A Non-Linear Material Coefficient	3.14
3.15	Phasor Relationship between the Real and Imaginary Components of Electrical Permittivity	3.16
3.16	Agilent Technologies Vector Network Analyzer.....	3.17
3.17	Cable Dielectric under Test in Dielectric Probe Fixture.....	3.18
3.18	Electrode for Clamp-on Cable Capacitance Measurement	3.19
4.1	Change in Storage and Loss Modulus after 50 Days at 140°C in Nitrogen, as Measured using DMA	4.1
4.2	DMA Plot after 17.8 Days at 160°C in Air.....	4.2
4.3	DMA Plot after 139 Days at 130°C in Air.....	4.3
4.4	Side-wall Reflections from Specimens 0 and 13	4.4
4.5	Plot of Indenter Modulus vs.....	4.5
4.6	Plot of Indenter Modulus vs.....	4.5
4.7	Top View and Side View of the Cable Specimen Used in the Guided Wave Inspection for Thermal Aging.....	4.6
4.8	Experimental Measurement Setup, and a Block Diagram Representing the Setup	4.7
4.9	2.54-cm Diameter Transducer Mounted on Top of an EPR Rubber Cable	4.7
4.10	Time Series Measurements with the Three Measurement Points for Cable C2 and Cable C10.....	4.8

4.11	Spectrogram of the Measurement Obtained at P1 on Cable Specimen C2.....	4.9
4.12	Wave Velocity Estimation for All the Nine Cable Specimens with Different Thermal Aging Times	4.9
4.13	Experimental Setup for Scanning the Pinducer Along the Surface of the Cable.....	4.10
4.14	Wavefront's Shape as they Propagate in Time, Obtained from the Scan Measurements.....	4.11
4.15	A Single Wavefont Extracted from the Image, and Its Linear Fit	4.11
4.16	Computed Wave Speed for the Three Cable Sections with Different Thermal Aging Times	4.12
4.17	Cable Housing Square Samples	4.12
4.18	Real Part of the Dielectric Constant for All Samples at 6000 MHz vs.....	4.13
4.19	Averaged Real Part of the Dielectric Constant at 6000 MHz vs.....	4.13
4.20	Mean Value of Real Part of the Dielectric Constant with Standard Deviation at 6000 MHz	4.14
6.1	LIRA Portable System for Assessing the Condition of Electrical Cables	6.2
6.2	An Example Impedance Spectrum which Forms the Basis for All Cable Evaluations Performed by Line Resonance Analysis	6.3

TABLES

3.1	Commercially Available Techniques for Cable Inspection	3.16
4.1	Summary of Cable Specimens and Aging Condition Used for Acoustic Measurements	4.6

ACRONYMS

DMA	dynamic mechanical analysis
DOE	U.S. Department of Energy
EAB	elongation at break
ECQCL	external cavity quantum cascade laser
EPR	ethylene propylene rubber
EPRI	Electric Power Research Institute
FTIR	Fourier Transform Infrared (spectroscopy)
IAEA	International Atomic Energy Agency
IR	infrared
LIRA	line resonance analysis
LWRS	Light Water Reactor Sustainability Program
NDE	nondestructive evaluation
NEUP	Nuclear Energy University Program
NPP	nuclear power plant
NRC	U.S. Nuclear Regulatory Commission
PNNL	Pacific Northwest National Laboratory
VNA	vector network analyzer
XLPE	cross-linked polyethylene

Assessment of Additional Key Indicators of Aging Cables in Nuclear Power Plants – Interim Status for FY2015

1. INTRODUCTION

The aging of insulation and jacketing material in electrical and instrumentation cables is considered to be one of the factors that may limit the ability of light water reactors to continue operations beyond their licensed period (up to 60 years, depending on the specific plant). The most important requirement for cables (power or instrumentation) in nuclear power plants (NPPs) is the ability to withstand a design-basis accident. Aging and consequent degradation of insulation will impair the ability of cables to perform their function under all environmental conditions. Methods to nondestructively assess the level of aging and degradation in cable insulation and jacketing materials are therefore needed. In addition to providing an estimate of the level of aging and degradation, such condition assessment or condition monitoring methods for cable insulation can also provide critical inputs into proposed condition-based qualification approaches (NRC 2013), assess corresponding remaining useful qualified life of the cable, and ensure that the cables do not exceed a qualified level of degradation.

1.1 Background

In July 2012, a workshop (Simmons et al. 2012) was held to lay the groundwork for a research and development roadmap to address aging cable management in NPPs, including methods for nondestructively measuring the condition of aging cables. This workshop brought together subject matter experts from the U.S. Nuclear Regulatory Commission (NRC), U.S. Department of Energy (DOE) national laboratories, the Electric Power Research Institute (EPRI), universities, and cable manufacturers and inspectors.

The workshop focused on identifying key research needs in the nondestructive evaluation (NDE) of aging cable insulation in NPPs and the associated technical gaps. Identifying measurable quantities from changes in chemical structure of insulating materials that would be a precursor to eventual failure of an aging cable, and state-of-the-art in NDE methods that could be applied to estimate the remaining life of the cable, were determined to be key to addressing the aging management challenge for nuclear cables. The changes in chemical structure are most likely to be caused by the environment the cable is in (with associated thermal, radiation, moisture, and chemical stressors) and the mechanical load (both static and dynamic) that is being applied. In turn, these changes in chemical structure are likely to result in corresponding changes in physical (including mechanical and electrical) properties of the insulation and/or jacket material. The development of new NDE methods or development of new measurement techniques using existing NDE methods that target these types of changes is of significant interest. Further, the ability to perform a nondestructive test to determine chemical, physical, mechanical, and electrical properties of the cable jackets and insulation without significant disturbance of the cables and connectors as they lay in-situ is essential.

There have been many programs and years of research to address the problems of aging nuclear cables (for instance, Yamamoto and Minakawa 2009; Villaran and Lofaro 2010; IAEA 2012) with no single NDE method identified that can satisfy all of the requirements needed to assess life expectancy. Currently, the gold standard for determining cable insulation degradation (through a measurement of cable elasticity) is the elongation-at-break (EAB) measurement. This is an ex-situ measurement and requires removing a sample of cable insulation for laboratory investigation.

The most common nondestructive methods used are visual (looking for cracking or discoloration indicative of cable aging) and a method that indents the surface of the cable jacket (measures cable elasticity and correlates to cable aging). In combination with visual and tactile assessments, the

indentation method is widely used to assess cable aging and degradation. The indentation method (Mantey and Toman 2013) is accepted by the nuclear industry as a nondestructive measurement of cable elasticity and has been correlated with EAB. However, the visual inspection and indentation techniques are applicable only to easily accessible cable sections. All other NDE techniques (such as time and frequency domain analysis, inductance and capacitance measurements, electrical tan δ , etc.) are used to find flaws in the conductor and do not readily provide information to determine the current health or life expectancy of cable insulation.

A related challenge to developing NDE methods is the development of associated acceptance criteria that define the threshold for degradation below which cables may continue to be used. EPRI Technical Report 1008211, “Initial Acceptance Criteria Concepts and Data for Assessing Longevity of Low-Voltage Cable Insulations and Jackets” (EPRI 2005) develops a basis for acceptance criteria and evaluates the aging profiles for many commonly used cable jackets and polymers. The report describes 50-percent EAB as a conservative practical end-of-life threshold for cables that may be stressed during maintenance or subjected to loss-of-coolant accident exposure. The report also discusses the basis for cautious continued use of cables beyond the 50-percent EAB threshold.

The 2012 workshop identified three important areas to be considered to assess overall cable aging:

1. Determine the key chemical, physical, and electrical indicators of cable aging.
2. Advance current and develop new NDE methods to enable in-situ cable condition assessment.
3. Develop models to assist in predicting remaining useful life of aging cables.

Figure 1.1 succinctly illustrates the importance of using NDE to predict remaining useful qualified life of aging cables and the individual properties that must be considered.

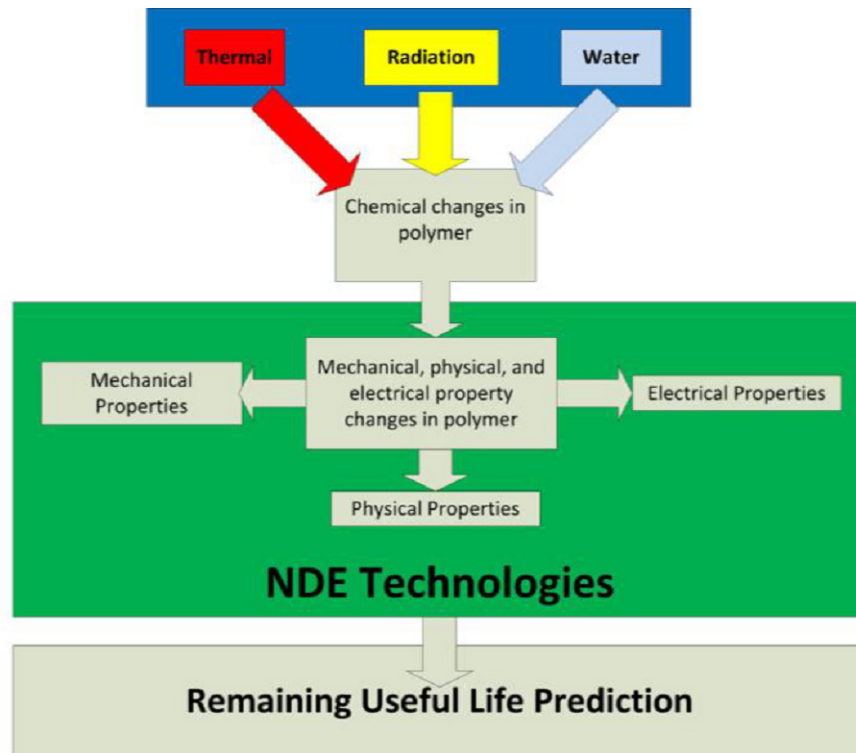


Figure 1.1. Overview of Research Tasks for Cable Aging Detection and Remaining Life Assessment

Subsequently (in late 2013 through early 2014), the research tasks listed in Figure 1.1 were integrated into a coordinated research plan jointly developed by DOE Office of Nuclear Energy (through the Light Water Reactor Sustainability Program [LWRS] program), the NRC, and industry (represented by EPRI). Several coordination meetings have taken place and the research activities under this integrated coordinated research plan have been shared and vetted among the lead research organizations.

Within the context of this project, developments from other research activities within this coordinated plan are leveraged for specimens, identification of key indicators, and access to measurement techniques. At the same time, results from this project are shared with the other activities for subsequent use in determining measurement techniques, analysis methods, and input into cable qualification techniques.

1.2 Overall Project Objectives

The overall objectives of this project are to develop the technical basis for assessing the level and impact of cable insulation aging and degradation in nuclear power plants. The project addresses the overall gaps that were identified at the workshop in FY2012 using a phased approach. This phased approach will address the three areas identified from the workshop, and listed above.

The focus of the project thus far has been on measurements of physical properties that act as key indicators of aging of ethylene propylene rubber (EPR)-insulated and cross-linked polyethylene (XLPE) cable, which are two of the primary cable material types used in NPPs. The overall objective of this effort is to complete an assessment of measurements of physical properties on cables subjected to a range of accelerated aging conditions (primarily thermal aging), and assess results for key early indicators of cable aging. The initial assessment evaluated available literature in current advances in polymer science to determine likely measurable conditions that can serve as key indicators of cable aging. In parallel, NDE measurement methods sensitive to these conditions as well as NDE methods currently being considered for cable aging assessment were identified to provide a foundation for further investigation.

The information presented in the following sections is based on the materials and conditions evaluated to date. Follow-on work will continue to assess NDE measurement methods, evaluate the potential of determining cable remaining useful life using the identified key indicators, and transition into advancing the state of the art in NDE methods that may be applied to in-situ assessment of the condition of cables. To assist in this effort, we continue (through the coordinated research work with the NRC and EPRI) to identify cables that can be (or have been) subjected to aging, measure physical properties of these aged cables using existing and possibly new NDE methods, and document results in upcoming technical reports.

1.3 Objectives of this Report

This Pacific Northwest National Laboratory (PNNL) interim report describes progress to date on investigating aging conditions that provide key indicators of cable aging and identifying measurement technologies that may be used as potential methods for examining cables. In addition to measurements on insulation materials, studies are also using cable systems (cable with conductor and insulator intact) for aging and NDE measurements. In addition to these measurements of key indicators (conducted ex-situ for convenience in a laboratory setting), in-situ measurements of other variables were also recorded using an energized cable that was simultaneously aged in a test-bed.

This report is the latest in a series of reports, each documenting studies on a subset of key indicators. Previous reports in this series focused on the evaluation of dielectric measurements and initial measurements of acoustic wave speed (Simmons et al. 2013). These measurements were made on aged EPR rubber (thermally aged at 140°C), and showed the feasibility of using dielectric measurements for assessing thermal degradation. A follow-on report (Simmons et al. 2014) provided additional confirmation of dielectric measurements, and demonstrated the feasibility of using measurements of elastic moduli (specifically the storage and loss moduli from DMA instrumentation, as well as sound

speed measurements on a subset of aged EPR material) to assess condition of aged EPR rubber. Likely key chemical indicators of aging (measured using FTIR, differential scanning calorimetry, and thermogravimetric analysis) also showed changes with thermal aging and were reported (Simmons et al. 2014). However, the use of a surface mounted interdigital capacitive probe was inconclusive, with respect to measurable trends with age.

The present document examines the ability to measure mechanical moduli using stress-wave-based interrogation methods, as well as the feasibility of applying higher resolution infrared (IR) reflectance spectroscopy. Supporting laboratory-based measurement methods that provide insights into the changes in material properties with thermal aging are also presented.

This report is submitted in fulfillment of deliverable M3LW-15OR0404022 “Complete Report Documenting Assessment of Additional Key Indicators of Aging Cable Insulation” (Level 3 Milestone).

1.4 Report Organization

This document is organized as follows. Section 2 summarizes the measurement needs from a materials science perspective. Specifically, the impact of degradation mechanisms of concern on materials microstructure and the key measurements that are needed for assessment of impact on structural integrity are summarized. Section 3 summarizes the leading candidates for nondestructive measurements that may be applicable to the problem at hand and describes the experimental approach. Section 4 summarizes the experimental data collected to date and describes the initial results of analysis of this data. Sections 5 and 6 summarize the findings to date and discuss the path forward. And Section 7 provides the references used in this report.

2. KEY INDICATORS OF CABLE DEGRADATION

The nuclear industry uses a variety of polymers and elastomers for insulators and jacketing materials with several of these materials often used in combination. A survey of the material types used as insulators and jacketing materials indicates that EPR and XLPE make up over 70% of the insulation material in U.S. NPPs (NRC 2013). Environmental qualification of cables for the nuclear industry uses a Class 1E qualification test that cables must be subjected to and that is in accordance with IEEE standards 323-2003 and 383-2003.

As cable insulation materials age and degrade, a technical basis for license renewal becomes necessary to provide reasonable assurance that the cables will function under all environmental conditions, including a design-basis-accident. EPRI document TR-103841, “Low-Voltage Environmentally-Qualified Cable License Renewal Industry Report; Revision 1” (EPRI 1994) provides a technical basis for license renewal for low-voltage environmentally-qualified cable. Specifically, the evaluation discusses age-related degradation mechanisms, the effects of age-related degradation on functionality of equipment, and aging management options. The nuclear power industry has considered age-related degradation mechanisms, but with a few exceptions, does not appear to have correlated these with NDE methods for periodic condition assessment or in-situ long-term condition monitoring.

The industry has accepted indentation modulus (EPRI 2005; Mantey and Toman 2013) as a key indicator and EAB as a measure of cable remaining useful life. Further, the indentation modulus has been correlated to the EAB. However, the indentation modulus is a localized measure of cable insulation degradation, requires physical access to the location for measurement, and measurements from one location cannot be readily extrapolated to assessing the condition of the cable over longer sections, especially in sections that are inaccessible and may experience different environmental conditions. EAB, on the other hand, is an ex-situ measure of cable remaining useful life.

Developing approaches for NDE that overcome the potential limitations of these methods will require a fundamental assessment of nondestructive measurements of physical, chemical, mechanical, and electrical properties for their sensitivity, reliability, and applicability to cable remaining useful qualified life estimation. The key to success in using these measurements in this project will be to understand the chemical changes that occur because of environmental stressors, and the effect of these changes on measurable properties of the insulator or jacketing materials.

Stressors —such as heat, radiation, and moisture— in a nuclear plant environment modify polymer chemistry and it is important to first understand the mechanisms involved in these changes. Previous studies have highlighted the role of oxidation as a key player in the aging and degradation of polymers exposed to heat and gamma radiation. Oxidation is a complex process involving several different chemical and molecular interactions. Degradation of cable is expected to vary significantly within a power plant because the stressor intensities vary widely within a containment structure.

Because control specimens of new vs. aged cable are limited or non-existent, specimens must be produced by accelerated aging techniques. The differences between degradation by accelerated aging and actual aging have been investigated by many researchers and a great number of results have been reported (IEC 1996; IAEA 2000; JNES 2009; Bowler and Liu 2015). Key observations relative to this study are:

- a. Degradation mechanisms above the melting point of XLPE and EPR can be fundamentally different from the degradation mechanisms below the crystalline melting temperature. Accelerated aging should be limited to thermal aging below the crystalline melting temperature to be consistently representative of aging within the nuclear power plants.

- b. At lower temperatures—below the crystalline melting temperatures—degradation is primarily associated with abstraction of hydrogen atoms from the polymer backbone and generation of reactive free radicals. These unstable species can react in a number of different ways to degrade mechanical performance including through chain scission, chain-cross-linking, de-polymerization, and related oxidation. This type of degradation, however, generally trends proportionally to the time and temperature exposure of the specimen.
- c. Radiation damage/degradation is also associated with free-radical generation and consequent chain scission, chain cross-linking, de-polymerization, and oxidation. Chain scission and chain cross-linking compete and the dominant process depends on degradation conditions including temperature and dose rate. When Kusano and Uno (2003) studied the mechanical properties of polyethylene (PE), the tensile strength of the PE specimens irradiated in vacuum first increased by more than 100 percent in response to a dose of 1.2 MGy, after which tensile strength decreased with increased dose. When Kusano and Uno (2003) radiated their samples in air, however, tensile strength decreased monotonically with increased dose. Because radiation dose is not necessarily directly proportional to mechanical performance, accelerated aging conditions should be kept as close as possible to in-plant conditions in terms of dose rates, temperature and oxygen atmosphere.

Factors that influence the aging and rate of aging include the composition of the materials involved, and their role in aiding or inhibiting aging-related polymer changes. The presence of multiple materials in a cable system (conductors, semiconductors, and insulators arranged in layers to form barriers to the external environment while minimizing electrical stresses during operation) may, on occasion, also impact aging rates and corresponding changes in the polymer chemistry. As a result, aging studies that include these other materials may provide additional insights into key indicators and likely NDE methods.

A previous interim report (Simmons et al. 2013) described the various chemical and physical properties that may be key indicators for cable insulation aging. Chemical indicators include changes in the levels of various additives, the level of crystallinity, the glass transition temperature, and the presence of reactive species, among other quantities. The result of chemical changes (such as chain scission or cross-linking) can affect physical properties such as strength, gas or liquid uptake, color, refractive index, elasticity, and electrical polarizability. Details of these changes, their causes, and the effect on the polymer, are available in Simmons et al. (2013).

NDE measurements that target these types of changes in the polymer are of interest, as they provide a measurable quantity that may be tracked over time to quantify aging and degradation in the cable. Further, by correlating these changes with EAB (the currently accepted gold standard for cable remaining life), the NDE measurement becomes a proxy through which remaining life of the aged cable may be estimated.

Nishida et al. (1999) describe results of studies correlating nondestructive measurements from aged polymers with EAB for a variety of nondestructive measurement methods. Measurements discussed include sound speed, stress-distortion response, twist-torque, rebound hardness, etc., and a range of polymer materials were studied. Many of these parameters appear to correlate well with EAB; however the correlation appears to be a function of material and aging type (thermal vs radiation).

A previous interim report (Simmons et al. 2013) described a number of nondestructive measurements that are likely to be sensitive to such key indicators of cable aging. In this report, additional studies focused on a few of these key indicators are described, along with an overview of ongoing research focused on laying the ground work for the next phases of research—advancing the state of the art in NDE for cables, and assessing remaining qualified life of aging cables.

3. EXPERIMENTAL ASSESSMENT OF KEY INDICATORS

A review of literature indicated several properties (physical, chemical, and electrical) of cable insulators that have the potential to serve as key indicators of aging-related degradation (Simmons et al. 2013; Simmons et al. 2014). Based on this survey, we selected a number of properties for initial assessment. The selection was based on the potential sensitivity of measurement techniques to the property, ease of obtaining measurements, potential for in-situ measurement, potential for developing measurement techniques that can interrogate the cable condition over longer distances, and availability of measurement equipment. This section describes the measurement techniques that are being evaluated experimentally for their sensitivity and reliability during this phase of the assessment. Additional properties (and related measurement techniques) will be evaluated in subsequent phases.

3.1 Materials

Two classes of insulators are being used in the studies on measurements of key indicators. The first of these is an ethylene propylene-based rubber material, typically referred to as EPR. The second material being studied is cross-linked polyethylene, referred to as XLPE. EPR and XLPE insulation are widely utilized in the nuclear power industry and comprise over 70 percent of the installed low-voltage cables in U.S. nuclear plants. These materials are available from a number of sources, and the materials and their sources selected were primarily for ease of procurement in addition to being among the major sources of cables in the nuclear industry. The differences between the selected materials and with other EPR/XLPE polymers are typically because of minor changes in the level or type of various additives, and the measurement techniques described and evaluated in this study are expected to be equally applicable to other similar polymers rubbers used in the nuclear industry.

EPR specimens used in this study were largely comprised of sections of cable (Figure 3.1) approximately 20 cm (8 in.) in length. Each cable section had a conductor roughly 16 mm (0.6 in.) in diameter, surrounded by a semiconductor tape and EPR insulation of ~5.5-mm (0.22-in.) thickness. In addition to the intact cable sections, some of the cable sections were used to extract the insulating material and fabricate EAB specimens. These specimens were heated in a forced air oven at different temperatures (140°C, 124°C, and 100°C). Specimens were removed at different time points and used in a number of the measurements described next. In addition, a longer section of cable [about 3.1 m (10 ft) in length, with a 60-cm (2-ft) section inside the furnace] was aged continuously at 140°C using the cable aging test-bed (Section 3.2). As the specimen set at 140°C comprises the most complete set to date, the bulk of the measurement data reported in Section 4 are on this set. Specimen aging at the other temperatures is ongoing, with a few specimens removed to date; data on these are reported where available with additional measurements and analysis forthcoming.



Figure 3.1. Photo of Cable with EPR Insulation for Use in Measurements of Key Indicators

The XLPE specimens used in this study comprised sections of cable approximately 60 cm (2 feet) in length. The cable sections had two conductors surrounded by the XLPE material; the insulator was surrounded by a shielding conductor which was, in turn, surrounded by a chlorosulfonated polyethylene (CSPE) jacket. In addition to the intact cable sections, tubes of the CSPE jacket (without the inner materials) and tubes of the XLPE insulation with the conductor removed were also used aged. These tubes (“straws”) will be used for measuring the EAB for these materials. Aging studies were being conducted at 100°C, with additional aging studies planned at higher temperatures (~125°C and 135°C).

In addition to the sections of cable, thin sheets (~1.6 mm in thickness) of EPR rubber (from the same source described earlier) were also used. Small sections (~1 cm × 1 cm squares) were cut from the sheets and aged at 140°C. In addition, some of these small sections were used in a dynamic mechanical analysis (DMA) tester under isothermal conditions to assess changes in elastic properties with aging.

3.2 Cable Aging Test-bed

PNNL has developed a test setup that can age the cable while cable property measurements are performed. The concept is to supply an operating voltage and current to an electrical cable that is representative of a cable used in a nuclear power plant, while it is being thermally aged in a forced-air oven. The cable remains in the furnace for the duration of testing and measurements can be made on the cable exterior to the oven. Figure 3.2 provides a graphic representation of the test apparatus and Figure 3.3 provides a photograph of the test setup assembled with a medium-voltage EPR cable.

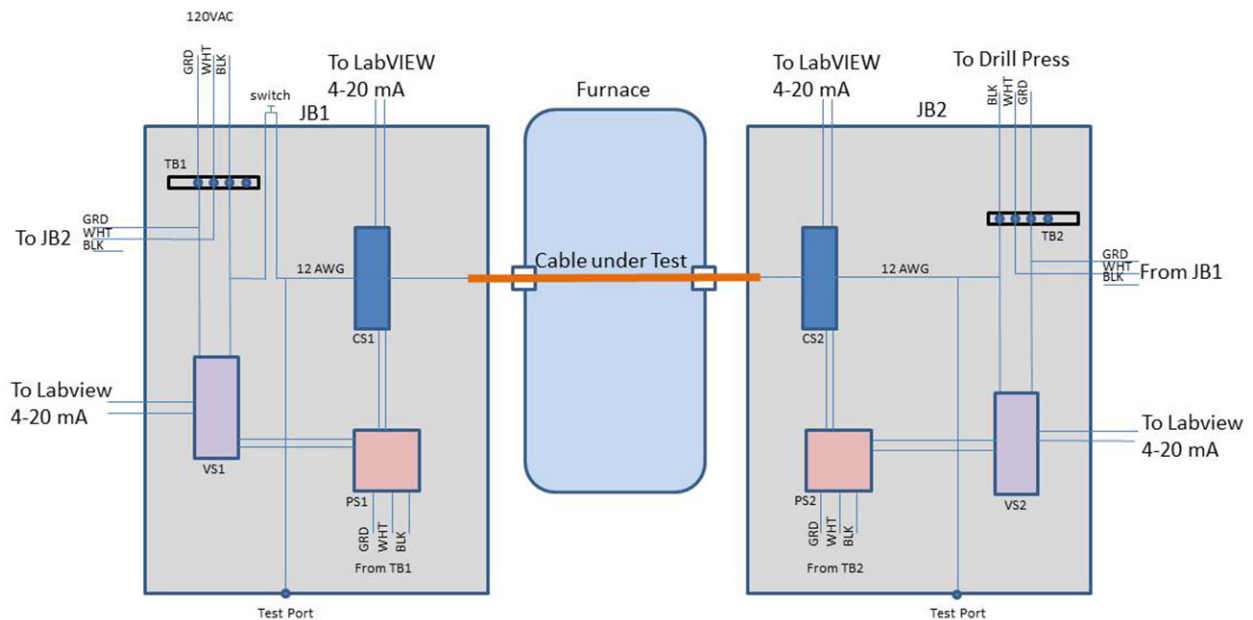


Figure 3.2. Graphic Representation of Measurement Circuit (where JB – Junction Box, TB – Terminal Block, CS – Current Sensor, VS – Voltage Sensor, PS – Power Supply)



(a)



(b)

Figure 3.3. Photograph Showing the Cable Aging Test-bed. The load (motor) is on the right of the oven and the Integrated Control System is on the left.

The cable is connected at one end to the wall outlet through a junction box. A load (in our case, a motor operating at 120 VAC, and drawing a maximum current of 7.5 A) can be connected to the other end of the cable through a second junction box, and turned on or off based on the test protocol. The circuit is monitored from a LabVIEW integrated control system (Figure 3.4), which allows measurements to be taken continuously at specified intervals. Temperature is monitored by eight thermocouples located both inside and outside the furnace, to ensure steady temperature and to track temperature shifts from the door being opened or possible power outages. An example of the data collected by the online-monitoring of EPR cable is shown in Figure 3.5.

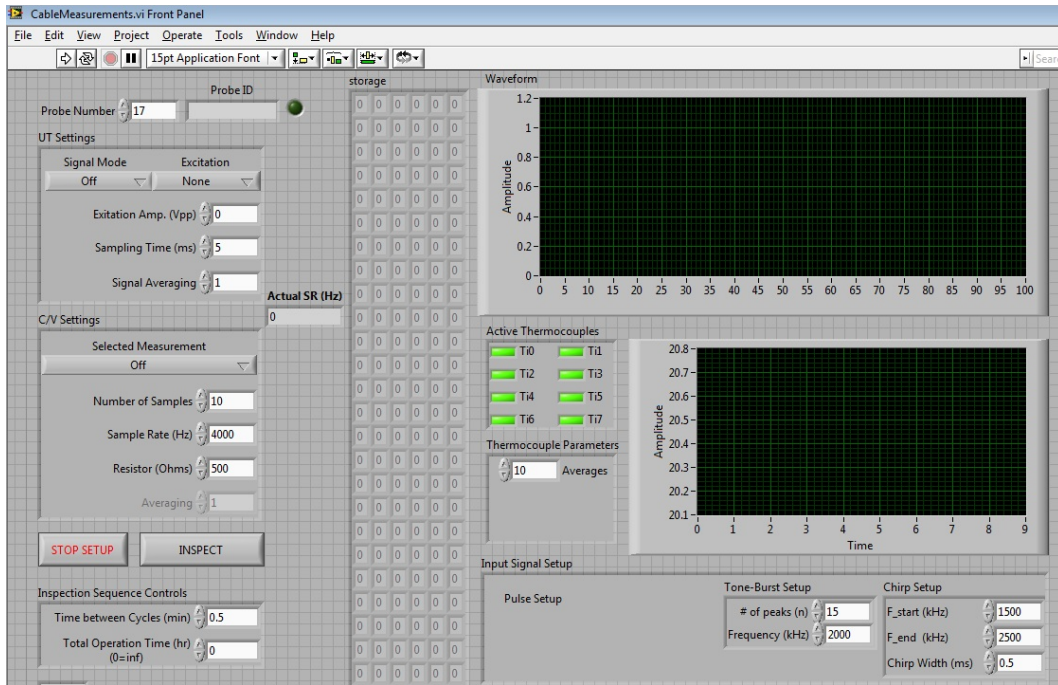


Figure 3.4. LabVIEW Integrated Control Interface

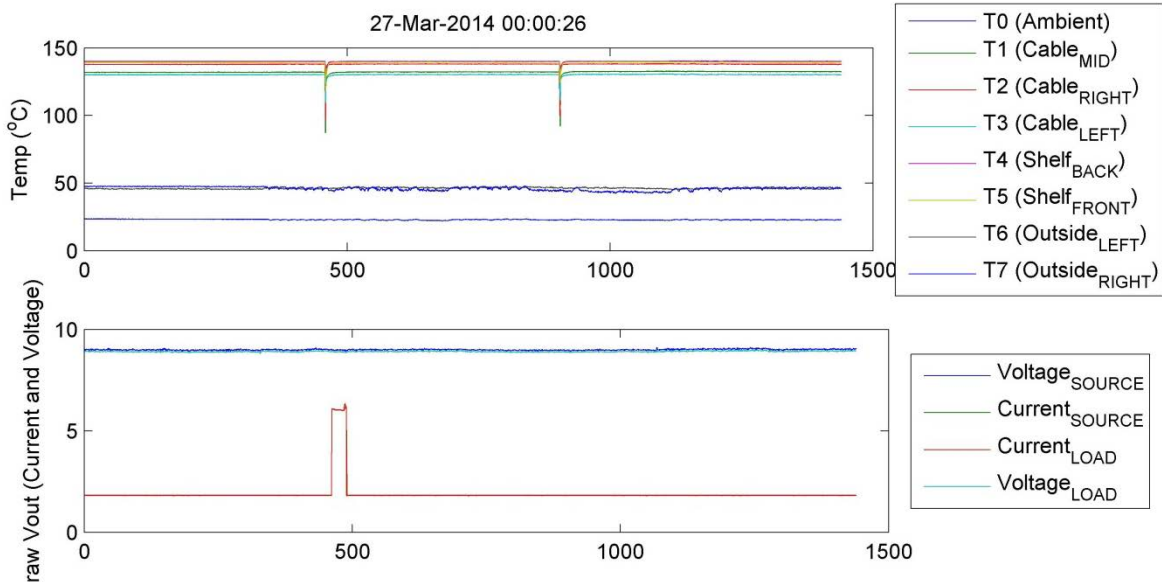


Figure 3.5. Representative Data Recorded by the Control System (x axis in minutes). Current spike is when drill is on. Temperature spikes are for opening door.

Additional test points are located in each junction box (input and output) to allow for additional (more precise) instrumentation to be added as needed. For the series of experiments conducted to date, voltage and current sensors were used to monitor the input and output voltages and currents as the load was cycled during the aging process. A rack that can hold up to 12 cable segments allows for simultaneous aging of smaller specimens for ex-situ nondestructive or destructive testing.

3.3 Measurement of Chemical Changes Using Infrared Spectroscopy

Chemical changes that polymers undergo with aging include oxidation, cross-linking, and chain scission. Polymer mechanical and electrical properties change with the chemical properties of polymer systems. As a result, analytical techniques are needed to determine the changes in chemistry to better form correlations with mechanical and electrical properties. An informative analytical technique for insulation material chemical property changes is infrared spectroscopy (Curl et al. 2010; Seguchi et al. 2011). Oxidation and cross-linking of cable insulation polymers such as EPR and XLPE inherently introduce new chemical bonds within the material, including C=O carbonyl and C=C carbon bonds, that have unique vibrational frequencies.

Given this, Fourier Transform infrared spectroscopy (FTIR) spectroscopy has commonly been used to characterize polymer degradation associated with these processes because the required equipment is widely available (Mailhot et al. 2004; Appajaiah et al. 2007; Namouchi et al. 2009). However, external cavity quantum cascade lasers (ECQCLs) may be relevant in these applications because of the extraordinarily high spectral resolution (less than 0.01 cm^{-1} in some cases) that they can deliver in regions ($3\text{--}19\text{ }\mu\text{m}$ typically) of the infrared where many unique absorption fingerprints can be found (Curl et al. 2010). Quantum cascade lasers are fitted with a so-called external cavity to achieve wavelength tuning for spectroscopy through a limited range. Although the resolution of ECQCL-based spectroscopy can be a substantial advantage in some applications, this weighs against the limitations of tuning range, which typically will not exceed a few hundred cm^{-1} . Thus, while the resolution bests that of FTIR, the user is limited to a narrow portion of the mid-IR spectrum.

To assess the ability to obtain high spectral resolution spectra (albeit in a narrow portion of the IR spectrum), an ECQCL was selected that had a tuning range of $1260\text{ to }1410\text{ cm}^{-1}$, corresponding to roughly $7.1\text{--}7.9\text{ }\mu\text{m}$ in wavelength units. Selection was driven by availability and by the fact that this range overlaps with at least one demonstrated EPR absorption line (as measured using FTIR transmission absorption spectroscopy). This is shown in Figure 3.6 for both aged and un-aged EPR cable sheathing material. We can see that there is a weak but well contrasted absorption line near 1380 cm^{-1} , which apparently disappears after aging. Therefore, the objective of this particular measurement was to determine if the same effect could be measured using a reflected beam from the ECQCL. This arrangement is expected to provide measurements that simulate FTIR reflection spectroscopy measurements (such as those obtained using hand-held FTIR instruments) but with higher spectral resolution and over a narrow portion of the IR spectrum.

Spectroscopy with ECQCLs has been applied to measurements of both gas-phase and solid-phase chemicals with great success. For transmission-mode measurements, the process of data interpretation is fairly straightforward, with the signals affected almost exclusively by light absorption. When opaque solid materials are used, however, the problem becomes significantly more challenging because the input spectrum is affected by both composition and sample morphology (Phillips and Bernacki 2012; Suter et al. 2012). Therefore, it can be difficult to predict what the reflectance spectrum from any given solid material will be when only the absorption from transmission measurements is known.

In this study, the incident ECQCL beam and the cable specimens were oriented in order to get as much of a “specular” reflection as possible into the photodetector. The cable was held in a rotating kinematic mount that allowed fine adjustment to get the maximum signal intensity from reflection. All free-space-optics were used for this experiment as shown in Figure 3.7. A half waveplate and linear polarizer were used to control the polarization of the incident light. In the experiments described in the subsequent section S polarization was used, meaning that the electromagnetic vector was perpendicular to the reflection plane.

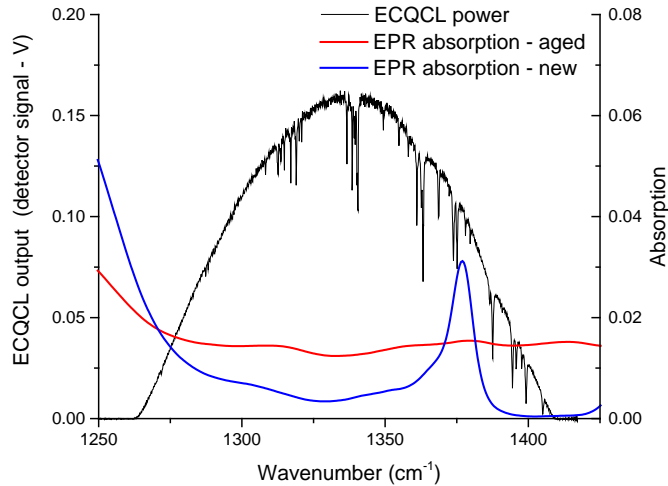


Figure 3.6. ECQCL Spectral Output Compared Against EPR Cable Material Pre- and Post-Aging, as Measured with FTIR Transmission. Note that the sharp dips in the ECQCL power spectrum are from atmospheric water absorption.

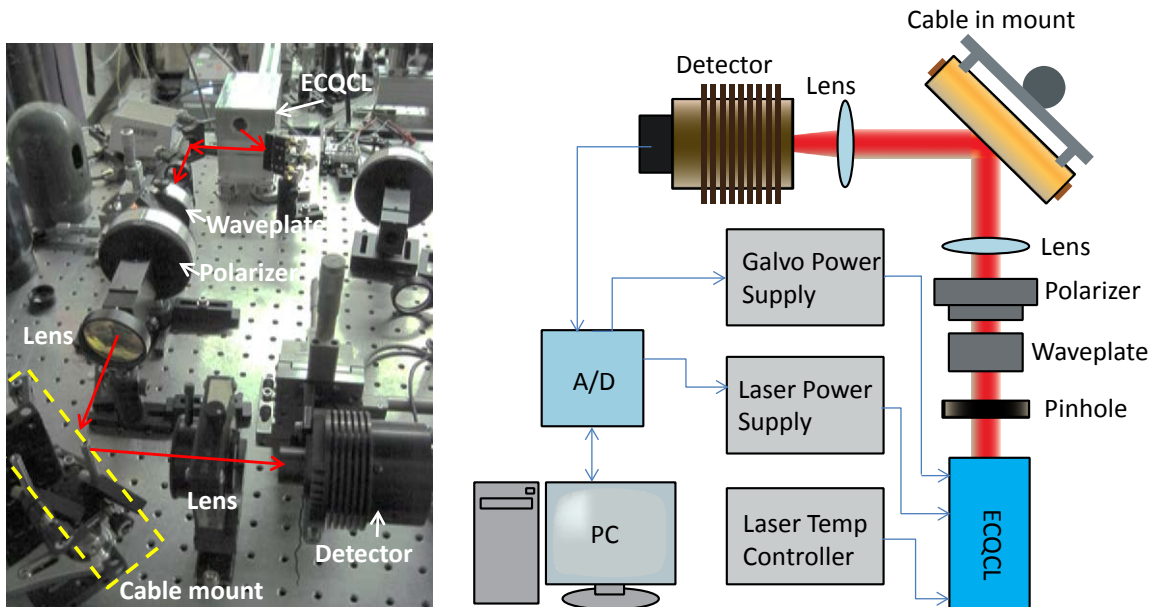


Figure 3.7. Photograph (left) and Schematic (right) of Cable Test Apparatus. Note that in the photograph the cable specimen is not present but its position is indicated with a yellow dotted outline.

A thermoelectrically cooled HgCdTe photodetector was used to collect reflection spectra. The laser was scanned over its entire tuning range using a turning mirror (this is the element that forms the proximal side of the external cavity), which was mounted on a motorized galvanometer dithered at 20 Hz. For noise and mode-hop suppression, the current controller for the ECQCL was also amplitude-modulated at 100 kHz. The scanning and modulation parameters were controlled through a National Instruments A/D board that provided access for the custom LabVIEW interface. This interface allowed the specification of scan range, modulation and scan frequency, averaging, and data saving specifications.

3.4 Measurement Techniques for Mechanical Properties

The most common measurement for sensitivity to aged conditions is destructive tensile testing known as elongation at break or EAB. Tensile strength may increase during initial aging and then dramatically decrease upon continued aging with some insulators. However useful in research, it is not practical to destructively test in-use cables for determining their aged condition (Gillen et al. 1999).

One of the key indicators that has previously been discussed (Yamamoto and Minakawa 2009) is the change in modulus of elasticity of the outer sheath material of a nuclear-grade cable. Aging of polymers used as cable insulation and jacket materials typically causes them to harden, thereby changing their elastic modulus.

Several approaches to measuring elastic modulus (or quantities that are related to the modulus) exist. The industry standard for measuring modulus is the indenter method (IAEA 2012), which is related to the elastic modulus. Studies indicate that the elastic modulus generally increases with thermal aging (Lofaro et al. 2001). Approaches besides the indenter method may provide greater sensitivity to changes in elastic modulus. These are described in greater detail below.

3.4.1 Indenter Modulus

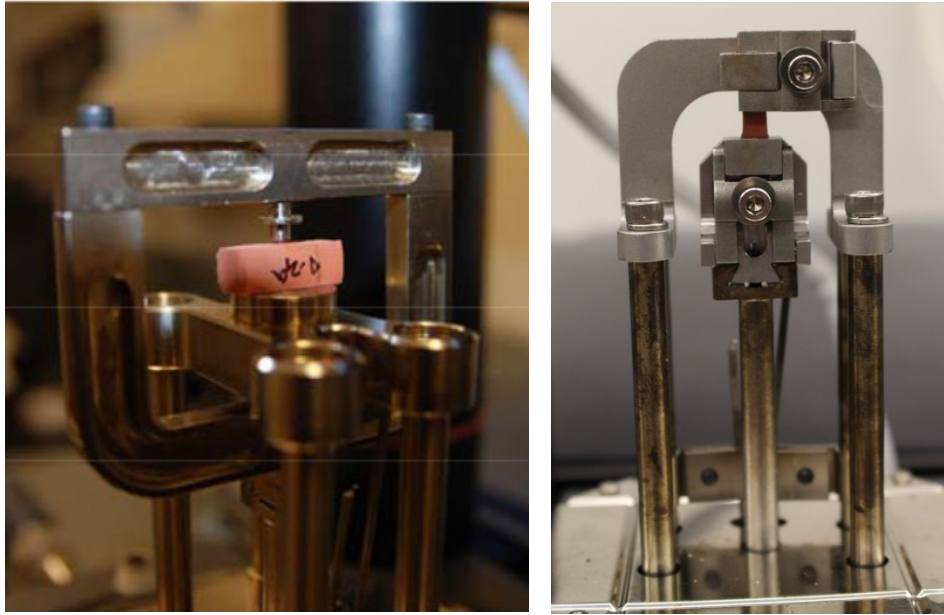
Nondestructive measurement of cable polymer material aging has been pursued through measurement of indenter modulus with commercial devices such as the Indenter Polymer Aging Monitor (IPAM) system (IEC/IEEE 2011). The indenter device clamps around a cable and presses a small probe tip against the cable at a constant velocity. The resistance to compression exhibited by the material being investigated on the surface of the cable can be correlated to the destructively obtained EAB. Advantages of this technique include its relative simplicity, its nondestructive nature, and the ability to perform the measurement in-situ. Disadvantages include its limitation to the outer surface of the intact cable, often consisting of a jacket rather than insulation, and the need to access the cable for the measurements.

3.4.2 Dynamic Mechanical Analysis

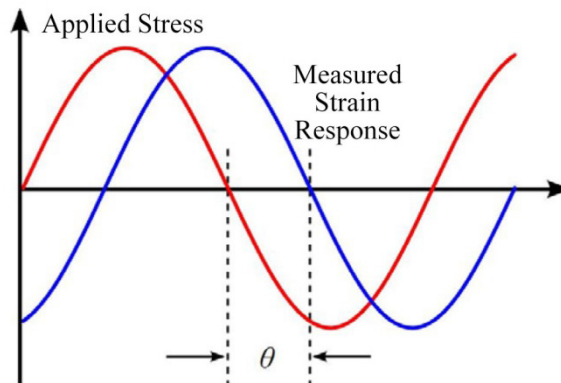
DMA is one of the techniques used to study the viscoelastic behavior of polymers (Menard 2008). DMA measurements typically apply a low-frequency (usually around 1 Hz) sinusoidal force (applied stress) and record the resulting response (measured strain) of the material. These data are used to compute the elastic (storage) modulus and loss modulus based on the lag between the applied stress and measured strain. While such measurements have been performed traditionally at a single temperature and frequency, the DMA instrument enables temperature sweeps temperature from -150°C to 150°C or higher at $2^{\circ}\text{C}/\text{min}$, as well as frequency sweeps to compute the dynamic behavior of the polymer.

Figure 3.8 illustrates how the system is configured to measure the material properties. The oscillating probe with its applied stress and measured strain compares the lag between the applied and measured conditions to calculate storage and loss moduli. The storage and loss moduli are the stored (elastic in-phase) and dampened (viscous out-of-phase) energy components, respectively. The ratio of the loss to stored moduli, a measurement of energy dissipation in the material, is the loss factor and is represented by $\tan \delta$. $\tan \delta$ is analogous to that of the electrical property measurements of which the ratio is a measurement of the lag between the applied and measured loads.

The test geometry can vary with tensile grips for specimens of thin geometries up to 3–4 mm (0.12–0.16 in.) in width. The shear stress mode using various probe tips can have different geometries depending on the stress level of interest. The studies reported here were performed on EPR cable material compound for testing, prepared from 15 cm \times 15 cm (0.6 \times 0.6 in.) sheets that were 1.5 mm (0.06 in.) thick. The DMA tensile mode specimens prepared from these sheets were 3 mm (0.12 in.) wide and 1.5 mm (0.06 in.) thick, and used a 0.91-mm (0.04-in.) probe diameter with right cylinder geometry. Cross-section specimens of \sim 5.5 mm (0.2 in.) thick and \sim 0.635 mm (0.03 in.) wide were cut from aged tensile specimens and subjected to DMA measurement conditions.



(a)



(b)

Figure 3.8. (a) Image of the DMA Instrument with Compression Tip for Shear Modulus (left) and Photograph of Tensile DMA Instrument Setup with Cable Insulation Specimen (right); (b) Illustration of Input/Output Waveforms that Form the Basis for the DMA Measurement

DMA measurements are sensitive to polymer transitions, levels of crystallinity, chain scission, and cross-linking (Sepe 1998). The DMA can be used to characterize material properties as a function of temperature, time, frequency, stress, and atmosphere. The DMA can also be used in thermomechanical analysis mode that can simulate not only the indenter test, but also look at mechanical stressors such as tensile, creep, and stress relaxation.

Figure 3.9 illustrates how information from DMA measurements can be used to compare changes in materials based on process conditions or changes in the polymer structure and morphology. The figure provides an overview of the types of changes in storage modulus expected from changes in polymer structure and chemistry that are typical of aging due to temperature and radiation. Given the types of information that are available from these measurements, it is apparent that DMA is an extremely valuable tool for polymer characterization.

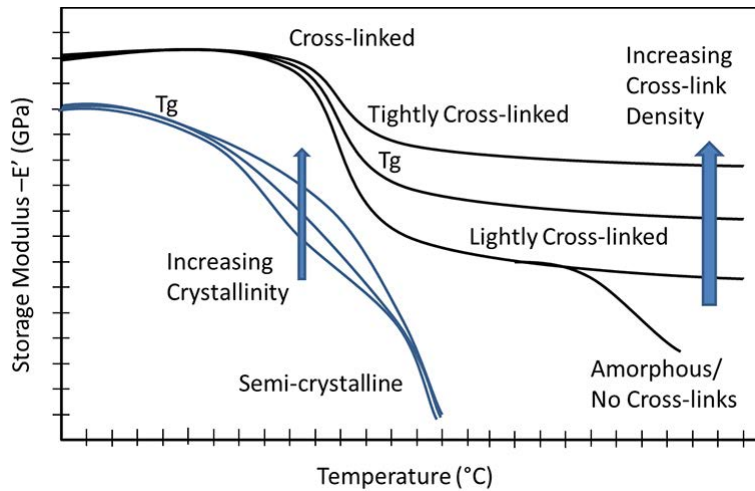


Figure 3.9. DMA Data Schematic Illustrating the Available Information Determined by DMA

DMA storage modulus data is related to stiffness of the material and hence its Young's modulus. This type of data is valuable for assessing techniques for acoustic measurements and the change in properties as it thermally degrades. In Figure 3.10, the DMA storage and loss modulus data from one formulation of EPR is shown in the baseline, un-aged condition. The data reveals a glass transition temperature of -48°C and very compliant soft material at room temperature relative to its high stiffness below the glass transition. The rise in storage modulus of this material with oven aging is illustrated in Figure 3.11.

In-situ testing of EPR, in which DMA tensile data are recorded continuously under isothermal conditions, was performed to monitor the material through its degradation cycle. Tests were performed in air at temperatures from 130°C to 180°C , and showed changes in sample length, storage modulus, and loss modulus with aging. Verification of the role of oxygen in the EPR aging was seen when aging in nitrogen atmosphere at 140°C revealed little change in the material. Details and the results of these tests are described in Section 4.1.

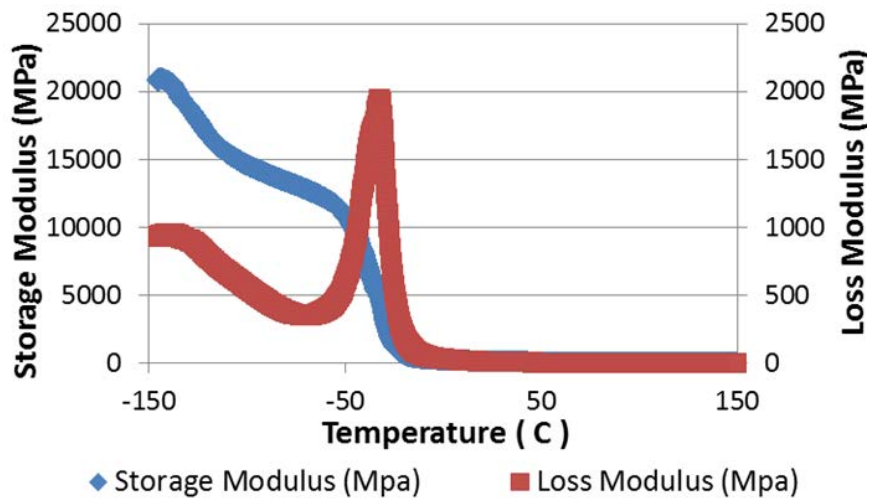


Figure 3.10. DMA Data for Un-aged Jumper Cable with EPR Insulation

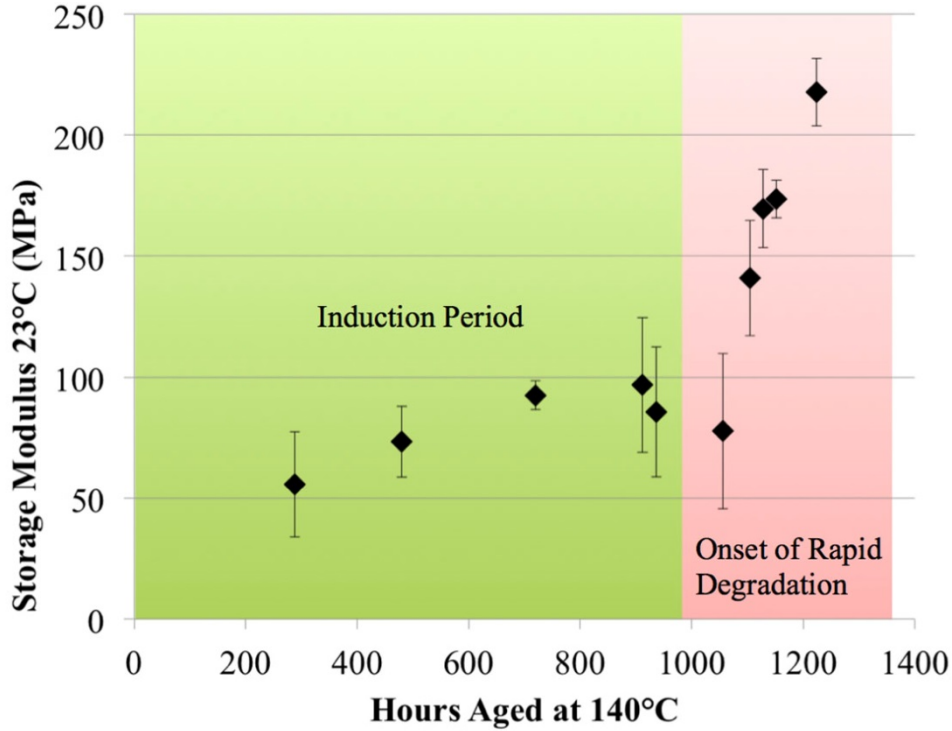


Figure 3.11. Storage Modulus of 140°C Thermally Aged EPR

3.4.3 Ultrasonic Measurements of Sound Speed and Attenuation

Acoustic wave interactions with solids depend on mechanical properties of the material (Pao 1983) such as density and elastic moduli (Krautkrämer and Krautkrämer 1990). In solids, these waves are also referred to as elastic or stress waves. The behavior of acoustic waves in solids is also a function of the wave mode. The three bulk wave modes usually considered are longitudinal or compressional (called L or P), horizontally polarized shear (SH), and vertically polarized shear (SV). In addition to these modes, surface and plate wave modes (and other modes) can also be generated, depending on the particular parameters and component geometry.

The wave speed c_l in solids for compressional waves is given by (Krautkrämer and Krautkrämer 1990):

$$c_l = \sqrt{\frac{E}{\xi} \frac{1-\mu}{(1+\mu)(1-2\mu)}} \quad (3.1)$$

and that of a shear wave is:

$$c_s = \sqrt{\frac{E}{2\xi(1+\mu)}}, \quad (3.2)$$

where E is the modulus of elasticity (units: N/m^2), ξ is the material density (kg/m^3), and μ is Poisson's ratio for the material (a dimensionless quantity). For plane waves or spherical waves, the sound pressure p (related to the applied force) and (compressional) displacement ζ are related by (Krautkrämer and Krautkrämer 1990):

$$p = \xi c_l \omega \zeta = Z \omega \zeta \quad (3.3)$$

where Z is the acoustic impedance.

These relations indicate that sound speed measurements may be a proxy to measuring the elastic modulus. When the velocity measurements are coupled with measurements of density of the medium, the resulting acoustic impedance of the medium may, in turn, be capable of providing a quantity that is, in form, similar to the indenter modulus. However, the ability to do so using acoustic methods may enable faster measurements of elastic modulus than can be made with the indenter method. Further, acoustic measurement of modulus may enable measurements over larger regions of the cable, something that requires manual positioning using the indenter method.

While the discussion above indicates that sound speed may be a relevant parameter because of its dependence on the elastic (Young's) modulus, the situation in polymers is somewhat complicated by their viscoelastic nature. In viscoelastic solids, the sound speed c and attenuation α may be expressed as (Theocaris and Papadopoulou 1978):

$$c = \left(\frac{|E^*|}{\xi} \right)^{1/2} \left(\cos \frac{\delta}{2} \right)^{-1} \quad (3.4)$$

$$\alpha = \frac{\omega}{c} \tan \delta \quad (3.5)$$

where E^* is the complex Young's modulus and $\tan(\delta)$ is the loss factor described earlier.

Literature indicates that acoustic methods have been evaluated to some extent and that good correlations exist between velocity and breaking elongation (Ikehara et al. 1998). A challenge with velocity measurements in polymers is the generally higher level of damping introduced by these materials, especially when using shear-wave transducers. Thus, initial trials have been focused on developing and refining the measurement protocol for longitudinal-wave velocity measurement in thermally aged EPR rubber.

Several approaches to measuring sound speed, as well as other acoustic parameters such as attenuation, are possible. In the longitudinal-wave approach, sound is propagated through the thickness of the specimen. The applied acoustic energy is reflected from the surfaces of the specimen (shown in Figure 3.12) and received by the transmitting transducer (or a second receiving transducer if one is used). The transit time through the thickness of the specimen (corresponding to an acoustic path length of twice the thickness) is generally used to compute the sound velocity. A delay line (such as an acrylic block) may be used to increase the standoff of the transducer from the specimen, and provide better separation of the responses from the near and far surfaces.

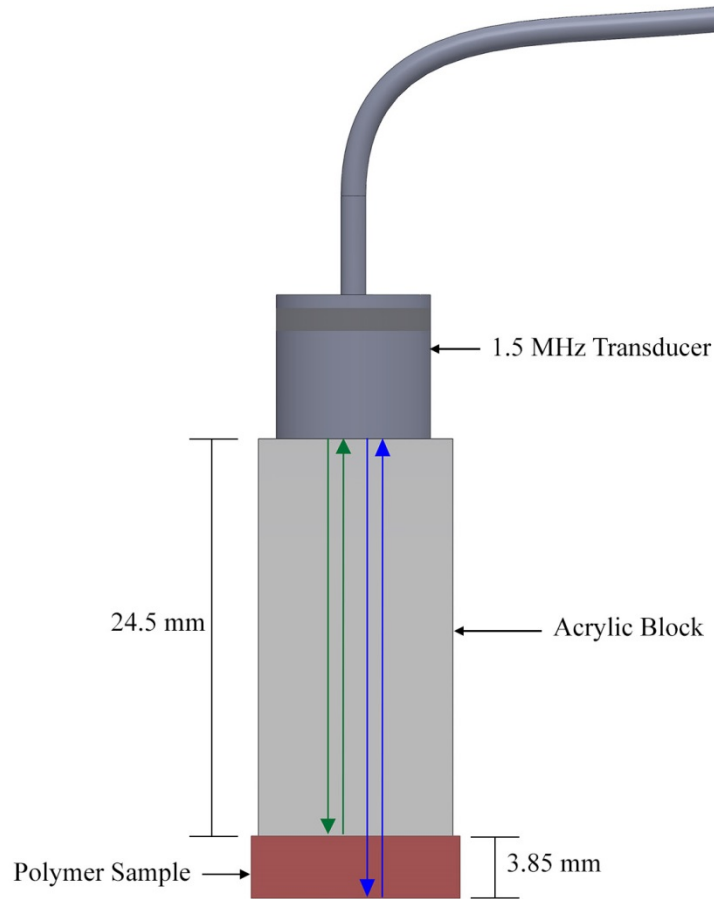


Figure 3.12. Ultrasonic Transducer Configuration for Standoff Measurement of Polymer Sample

An alternate approach to measuring bulk wave speed is described in Nishida et al. (1999), and uses two ultrasonic transducers mounted on angled wedges and separated by some distance. One of the transducers is used as the transmitter, while the second transducer acts as the receiver and measures the arrival time (relative to the transmitted time) of the acoustic wave. Sound speed is then estimated as:

$$c = \frac{L_2 - L_1}{t_2 - t_1} \quad (3.6)$$

where c is the acoustic wave speed, L_1 and L_2 are displacements between the transducers parallel to the cable axis, and t_1 and t_2 are the time-of-flight arrival times of the acoustic signal for the two displacements, respectively.

This approach, while conceptually simple, can suffer from uncertainty in a number of factors, including uncertainty in determining the correct incident angle, coupling inconsistency between measurements, variation in sound speed because of material aging and in various classes of insulation material, etc. These same uncertainties are likely to negatively impact measurements of acoustic attenuation as well as other acoustic measurements. Options for mitigating these issues include non-contact measurements and the use of dry coupling techniques (Owens et al. 2005).

Surface waves (also known as Rayleigh waves) differ from bulk longitudinal and shear-wave modes in that the waves follow the contour of the surface and penetrate the medium to only about one wavelength deep from the surface (Roberts 1990; Ensminger and Bond 2011). The velocities of Rayleigh surface waves c_R , bulk longitudinal waves c_l , and shear waves c_s are related by Ensminger and Bond (2011):

$$\frac{c_R^6}{c_s^6} - 8 \frac{c_R^4}{c_s^4} + c_R^2 \left(\frac{24}{c_s^2} - \frac{16}{c_l^2} \right) - 16 \left(1 - \frac{c_s^2}{c_l^2} \right) = 0 \quad (3.7)$$

An approximate value for the Rayleigh wave velocity was given by Viktorov (1967)

$$c_R = c_s \frac{(0.87 + 1.12\mu)}{(1 + \mu)} \quad (3.8)$$

where μ is Poisson's ratio.

There are four popular methods that can be used to generate surface waves in solids which have been described by Rose (2004):

1. A normal beam transducer directly placed on the surface. This is the simplest method; however, the wave propagates in both directions on the material surface.
2. A comb transducer, which is composed of a periodic array of piezoelectric elements. To generate surface waves, the spacing between the elements should be half the wavelength of the Rayleigh wave.
3. A normal beam transducer on a wedge, with the transducer oriented at an angle with respect to the material surface. The wedge angle is such that wave going out of the wedge into the material is converted into a surface wave according to Snell's law. In this method, the wave propagates only one direction. However, for the material considered in this study, the anticipated wave speeds are much lower than those in Plexiglas® (poly(methyl methacrylate)) or Rexolite® (polystyrene), which are typical materials used for wedges. According to Snell's law, surface waves cannot be excited in this situation.
4. A normal beam transducer on a wedge, which is bonded to a steel mediator. A surface wave is excited in the mediator, which has a sharp edge touching the solid; thus, "mediating" the transfer of the surface wave into the solid of interest. This solves the problem of having the wedge placed directly on the material surface, and also allows the wave to propagate in one direction. However, the probe design becomes more complicated.

For the materials used in this study, several challenges exist with respect to measurement of sound velocity. Accurate measurement of longitudinal-wave velocity requires precise knowledge of the thickness of the insulation. However, the as-fabricated cable sections have variable thickness of insulation (although still within tolerances necessary for nuclear power plant application). Specifically, the thickness varied across cable sections, with standard deviation of insulation thickness across all specimens being 0.235 mm (in a nominal thickness of about 5 mm (0.2 in.)). This variation (and the difficulty in precise measurement of thickness at arbitrary locations on the cable section) results in a corresponding variability in the calculated wave speed. This variability was observed in initial measurements of the longitudinal-wave velocity in EPR sheets (Simmons et al. 2014).

The surface-wave method does not require knowledge of the material thickness, because it allows measurement of the wave at two points with a well-known separation on the surface of the material. Then the difference in the time of flight between those two points directly gives the wave velocity. Moreover, it allows measurement of a long section of a cable at once, rather than a single point. To allow waves to propagate long distances along the cable with sufficient energy, operating in the low-frequency regime is required. The main challenge is the complexity of the received signals, and advanced signal processing methods are required to extract time-of-flight information from the measurements.

3.4.4 Non-Linear Ultrasonic Measurements

Another approach for characterizing materials is non-linear acoustics. When an acoustic wave propagates through a non-linear medium, the transmit wave is transformed into a distorted wave with higher harmonic components. Typically this wave has energy at integer multiples of the transmitted wave but is dominated by the wave's second harmonic occurring at twice the frequency of the primary transmit wave (Figure 3.13).

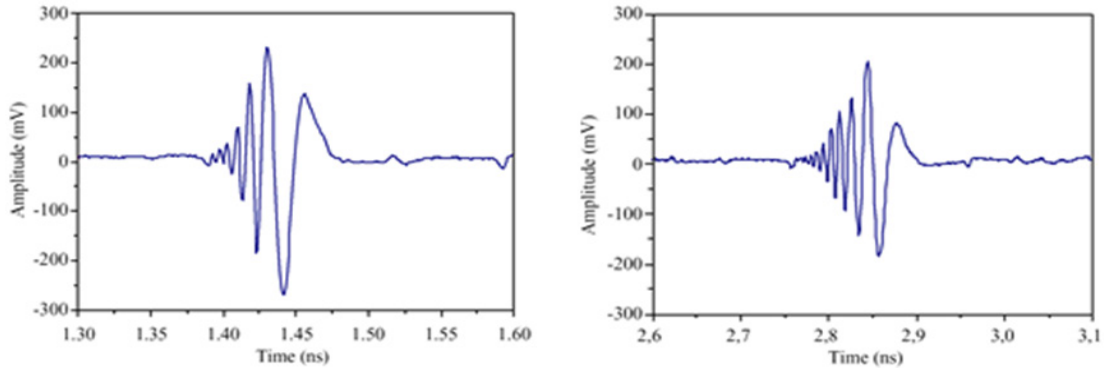


Figure 3.13. Non-Linear Media Affected Signal (right) Compared to Initial Signal (left)

The traditional measure of this non-linearity is a sound-path normalized expression of the second harmonic distorted signal compared to the first harmonic. This is referred to as B/A. The B/A term is a known value for a number of materials including biological tissue samples, water, oil, and other media. In medical diagnostics, this term is widely used to sense subtle changes in the tissue's mechanical and elastic properties that seem closely related to the parameters of interest in the cable insulation. Measurement of the B/A term can be performed by a finite-amplitude through-transmission method as illustrated in Figure 3.14.

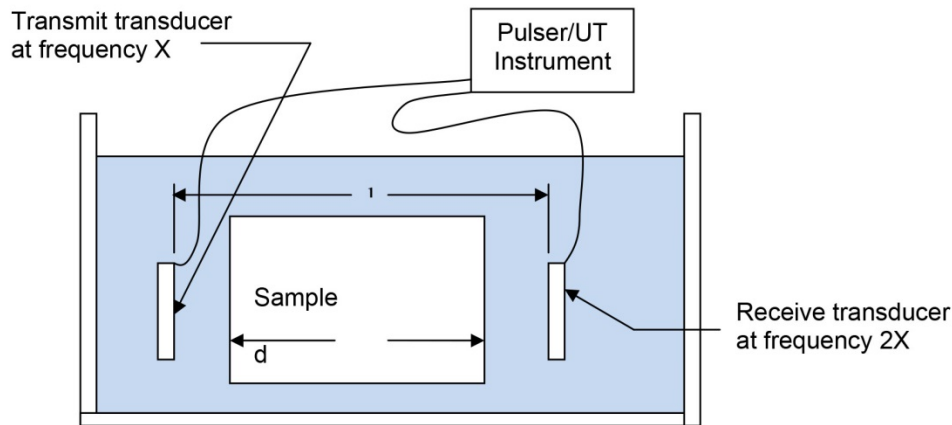


Figure 3.14. One Test Configuration for Measuring B/A Non-Linear Material Coefficient

The finite-amplitude through-transmission method measures B/A of the sample by using two unfocused transducers, one transmitting with a center frequency of X MHz and one receiving transducer with a center frequency of 2X. Using the two opposing transducers, transmitted signals may be recorded with and without the sample in the acoustic path. The non-linear parameter $(B/A)_s$ of the sample is then determined by using the following

$$(B/A)_s = \left\{ \left[\left(\frac{A_{2s}}{A_{2w}} \right) \left(\frac{L}{d} \right) - \left(\frac{L}{d} - 1 \right) \exp(-2\alpha_2 d) T_{ws} T_{sw} \right] \times \frac{\rho_s c_s^3}{\rho_w c_w^3} \frac{d}{T_{ws}^2 T_{sw}} \frac{2\alpha_1 - \alpha_2}{\exp(-2\alpha_2 d) - \exp(-2\alpha_1 d)} \left[(B/A)_w + 2 \right] \right\}^{-2} \quad (3.9)$$

where the subscript s refers to the sample and the subscript w refers to the degassed water. A_{2s} and A_{2w} are the amplitudes of the second harmonic of the transmitted signals with and without the sample in the acoustic path, respectively. L is the distance between the two transducers and d is the sample thickness. α_1 and α_2 are the attenuation coefficients of the sample at the first (1X Hz) and the second (2X Hz) harmonic frequencies, respectively. ρ is the density and c is the sound speed. Note that the density of the sample (ρ_s) was taken to be the density that was determined from separate measurements of the wet weight and volume of each sample. $(B/A)_w$ is the non-linear parameter of distilled water (approximately 5.2 at 20°C) (Lee 2013). $T_{ws} = 2\rho_s c_s / (\rho_w c_w + \rho_s c_s)$ and $T_{sw} = 2\rho_w c_w / (\rho_w c_w + \rho_s c_s)$ are the transmission coefficients at the water/sample and the sample/water interfaces, respectively.

The test described above would be impractical to perform for cable in the field however a similar dry test is envisioned for in-situ cable characterization to measure a parameter proportional to B/A subject to limitations of an adequate signal in the highly attenuative material, normalization for temperature variations, and adaptation of the reference B/A for a dry test. The principle advantages of this test will be the relative independence of the measurement on knowing the exact cable insulation thickness.

3.5 Measurement Techniques for Electrical Properties

As described in Simmons et al. (2014), a number of resources, such as the International Atomic Energy Agency (IAEA) Nuclear Energy Series *Assessing and Managing Cable Aging in Nuclear Power Plants* (IAEA 2012) and the *Light Water Reactor Sustainability (LWRS) Program – Non-Destructive Evaluation (NDE) R&D Roadmap for Determining Remaining Useful Life of Aging Cables in Nuclear Power Plants* (Simmons et al. 2012), were used to assess the state-of-the-art in NDE methods for measuring electrical properties of degraded cables. Table 3.1 (reproduced from Simmons et al. 2014) identifies commonly used electrical measurements and their advantages and disadvantages. The main advantage to electrical measurements is the possibility of evaluating the entire cable length in-situ. The main disadvantage is that they are often not very sensitive to insulation degradation.

The basic criterion for selecting methods for further assessment in this study was the requirement that the method must have the ability to perform a nondestructive test to determine electrical properties of the cable jackets and/or insulation without significant disturbance of the cables and connectors as they lay in-situ. Each of the electrical methods described in the table was considered intrusive in that one or both ends of the cable would have to be disconnected. The process of disconnection and reconnection of cables introduces opportunities for errors that may impact the associated circuits; as a result, in-situ methods are preferred.

With the exception of reflectometry (ideal for identifying faults in the conductors in cables) and partial discharge (which may, under certain conditions, result in added degradation to the cable insulation), the remaining methods in Table 3.1 each can potentially be used in-situ. As described in previous reports in this series (Simmons et al. 2014), dielectric measurement techniques were selected for initial evaluation because of their potential for in-situ evaluation. Other techniques, including recent developments in reflectometry-based measurements that may provide increased sensitivity to insulation degradation, will be examined in the next phase.

Table 3.1. Commercially Available Techniques for Cable Inspection (from Simmons et al 2014)

Inspection Method	Advantages	Disadvantages
Time-Frequency Domain Reflectometry (TDR and FDR)	Commonly used for determining the condition of instrumentation, control, and power cables where they are inaccessible.	Currently intrusive, requires disconnecting the cables to install instrumentation.
Insulation Resistance	Commonly performed in industry to determine the condition of the cable insulation.	Currently intrusive, requires disconnecting the cables to install instrumentation.
Inductance/Capacitance/Resistance (LCR)	Good for detecting changes in electrical circuit (cable and termination) by trending changes in inductance, capacitance, and resistance.	Currently intrusive, requires disconnecting cable at one end. Does not indicate location or cause of change in measurement.
Tan Delta ($\tan \delta$)	Determines changes in insulation (dielectric) properties by measuring change in dielectric loss angle. Can measure aging effects over entire cable length.	Intrusive, requires decoupling both ends. Single number from long cable makes isolating location of aging section difficult. Loss angle may be trended; however, single measurement insufficient to estimate remaining life.
Partial Discharge	Good for determining voids or defects in insulators of medium-voltage cables.	Test can damage the insulator with localized heating that causes degradation.

FDR = frequency domain reflectometry
 LCR = inductance/capacitance/resistance
 TDR = time domain reflectometry

3.5.1 Tan δ Measurement Technique

The dielectric measurement technique (often known as the tan delta technique or $\tan \delta$) can be derived from one of Maxwell's four equations, which relates the magnetic field intensity to the electric field intensity. The complex electrical permittivity of materials can be written as $\epsilon_r = \epsilon_r' - j\epsilon_r''$ and shown on a simple phasor diagram (Figure 3.15).

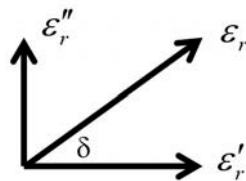


Figure 3.15. Phasor Relationship between the Real and Imaginary Components of Electrical Permittivity

The tangent of the angle δ between them is a measure of the ratio of energy from the applied electric field that is stored in a specific material to the amount dissipated or lost. This quantity is known as the loss tangent and defined as:

$$\tan \delta = \frac{\epsilon_r''}{\epsilon_r'} \quad (3.10)$$

for that material.

The measurement of the complex permittivity is typically performed using coaxial probes or capacitive probes.

3.5.1.1 Coaxial Dielectric Probe Technique

To understand the fundamental relationship between aged samples of electrical cables, PNNL employed a vector network analyzer (VNA) to acquire complex permittivity measurements. The VNA used was an Agilent Technologies model E8361A with integrated software and an associated high-temperature coaxial dielectric probe with a frequency bandwidth of 200 MHz to 20 GHz as shown in Figure 3.16. The VNA applies a known small sinusoidal electric field input to the material under test and measures the response of the material, including the amplitude and phase lag of the response relative to the applied input. Sweeps of frequency over the bandwidth of the probe are commonly performed and provide information on the variation of the permittivity with frequency.

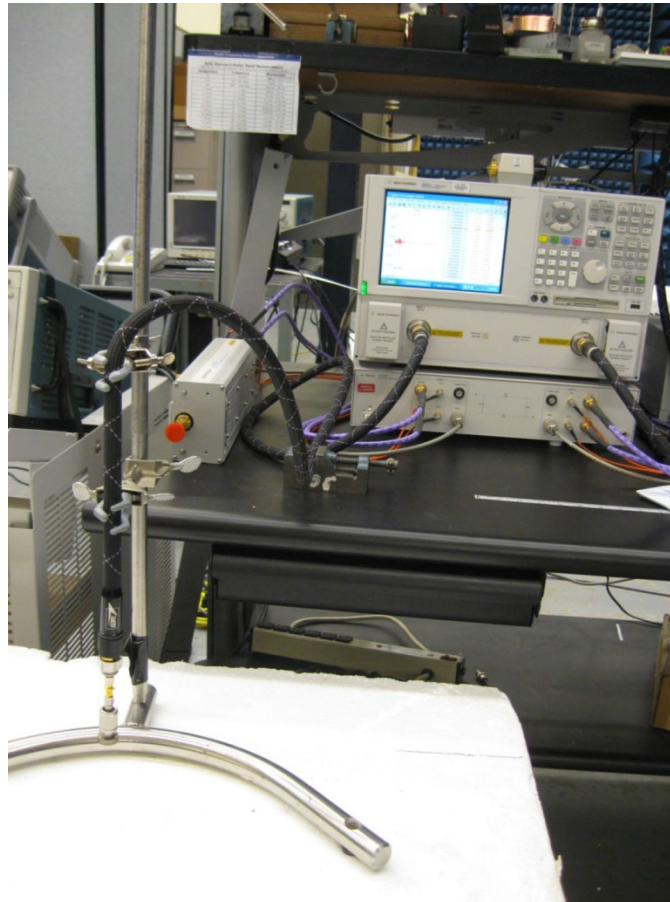


Figure 3.16. Agilent Technologies Vector Network Analyzer

Calibration of the VNA is essential to assure accurate, repeatable measurements of the complex permittivity. Calibration of the VNA is performed by subjecting the measuring probe to air, shorting the probe using a short-circuit standard, and then placing the probe in deionized water at a reference temperature. The reference temperature was 23°C for these measurements. Once calibration was completed, measurements of the complex permittivity of known materials (such as air and Rexolite®) were used to verify the accuracy of the calibration.

Complex permittivity measurements were performed on aged cable specimens to determine if there is a measurable trend in the change in dielectric constant vs. cable aging. These measurements were primarily conducted with cable segments and thin sheets of the cable insulation that were representative of different physical ages by aging the specimens at 140°C for different durations. The specimens under test were then placed inside a test fixture in which the specimen is clamped against the probe to provide consistent contact pressure between the probe and the cable housing (see Figure 3.17).

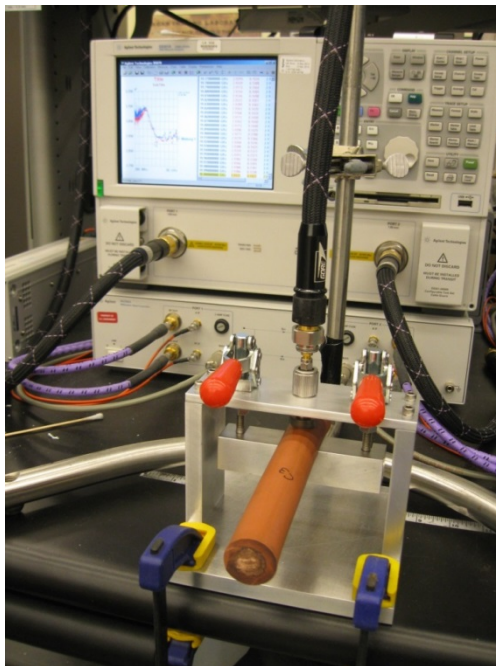


Figure 3.17. Cable Dielectric under Test in Dielectric Probe Fixture

3.5.1.2 *Capacitive Measurements*

Initial studies using an interdigital capacitive probe provided no clear direction trends in measurements with aging of EPR insulation (Simmons et al. 2014). This may be because of a number of factors, including low sensitivity of the probe and insufficient change in dielectric parameters with EPR insulation under the aging conditions explored to provide significant change in the capacitive measurement. Recent studies appear to indicate that suitably designed capacitive probes may be capable of sensitivity to thermal aging in EPR and XLPE insulation (Sheldon and Bowler 2013). An interdigital sensor electrode is affixed to opposing faces of a foam-padded hinged jaw clamp. The clamp with the foam backing on the jaws presses the electrodes onto the insulation surface (Figure 3.18). The measurement determines the capacitance and dissipation factor associated with insulation plus its conductor at the location of the clamp. These measurements have been shown to vary as a function of the polymer condition. PNNL recently began collaboration under the Nuclear Energy University Program (NEUP) with Iowa State University, where the university partner is exploring this technology and attempting to assess sensitivity to thermal, radiation, and synergistic aging of EPR and XLPE insulation. As they become available, results from this collaborative effort will be incorporated, as appropriate, into planned research at PNNL under the LWRS program on advancing the state-of-the-art NDE methods.

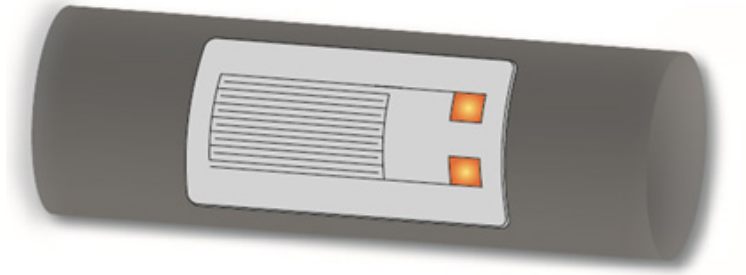


Figure 3.18. Electrode for Clamp-on Cable Capacitance Measurement. A spring-loaded clamp with a foam substrate (not shown) assures a good fit of the electrode to the insulation face.

4. RESULTS

The measurement techniques described above were used to acquire data on specimens of un-aged and aged EPR rubber, described in Section 3.1. The electrical measurement protocol is relatively mature, and was used previously to perform measurements and analysis on a set of un-aged and aged EPR specimens. These were reported in a previous report in this series (Simmons et al. 2014). In this section, the correlation of these measurements with other types of measurements is described, as are the data from other types of measurements (DMA, acoustic measurements, and infrared spectroscopy).

4.1 DMA Measurements

DMA tensile mode was evaluated as a new technique to simulate tensile modulus changes using isothermal temperatures and by monitoring the storage modulus as a function of time. The method was also evaluated using nitrogen gas to determine the impact of thermal stress in the absence of air. Figure 3.8 illustrates the tensile specimen behavior in the DMA.

The specimen geometry is 3-mm wide and 1.5 mm-thick with an overall length of 15 mm. The gap between the grips is ~10 mm. A series of frequency and strain sweeps were performed to determine the optimum range in frequency and amplitude for the test. The optimum values were determined to be 1 Hz frequency, 10 microns in amplitude, and stress of less than 1 MPa. The first temperature evaluated was 140°C in nitrogen gas and the test ran for 50 days (1200 hours). Figure 4.1 illustrates a minimal change in the storage modulus after 50 days. The storage modulus increased by less ~25%. Typical EAB results after exposures at the same test temperature and time in air would be below 50%. The results were quite revealing as to the impact without atmospheric air. There were no significant changes to the properties of the material.

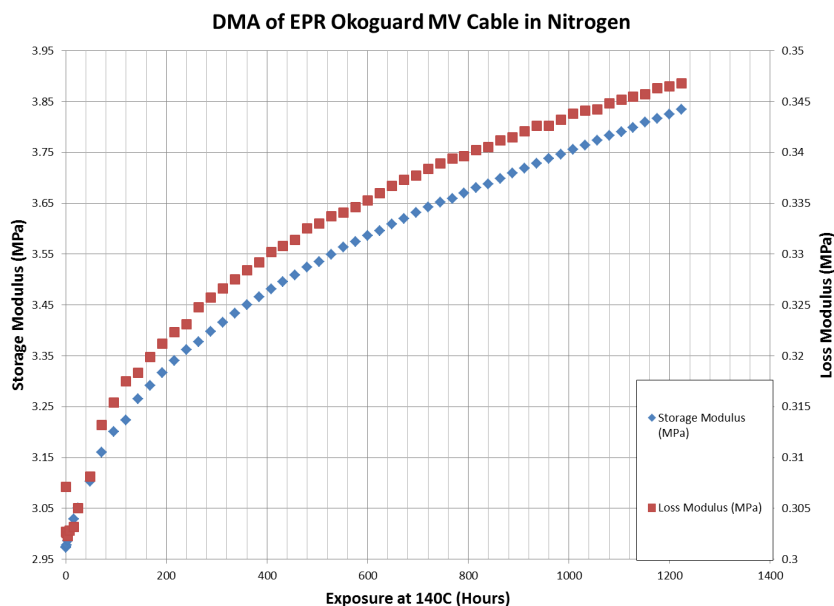


Figure 4.1. Change in Storage and Loss Modulus after 50 Days at 140°C in Nitrogen, as Measured using DMA

In the in-situ measurement plots (Figures 4.2 and 4.3), EPR specimens were held 160°C and 130°C isothermally and aged in air. The temperature differences resulted in nearly an order of magnitude difference in time to failure for the specimens. The figures show the storage and loss moduli, as well as the displacement and tan δ as a function of hours aged, for EPR aged at these two temperatures. Changes in the slope of the tan δ values indicate changes in the geometry of the specimens (such as specimen elongation and sample cracking). Collectively, these three studies point to the possibility of using mechanical measurements for assessing EPR sample age, assuming aging in air.

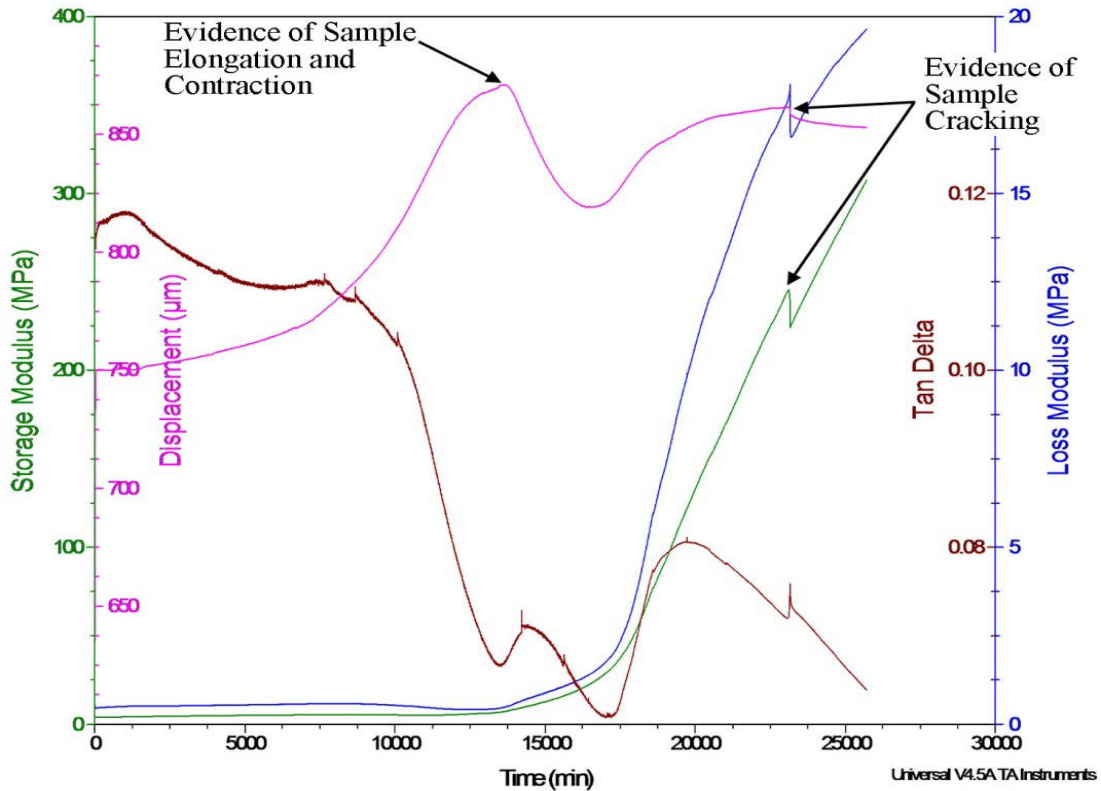


Figure 4.2. DMA Plot after 17.8 Days at 160°C in Air

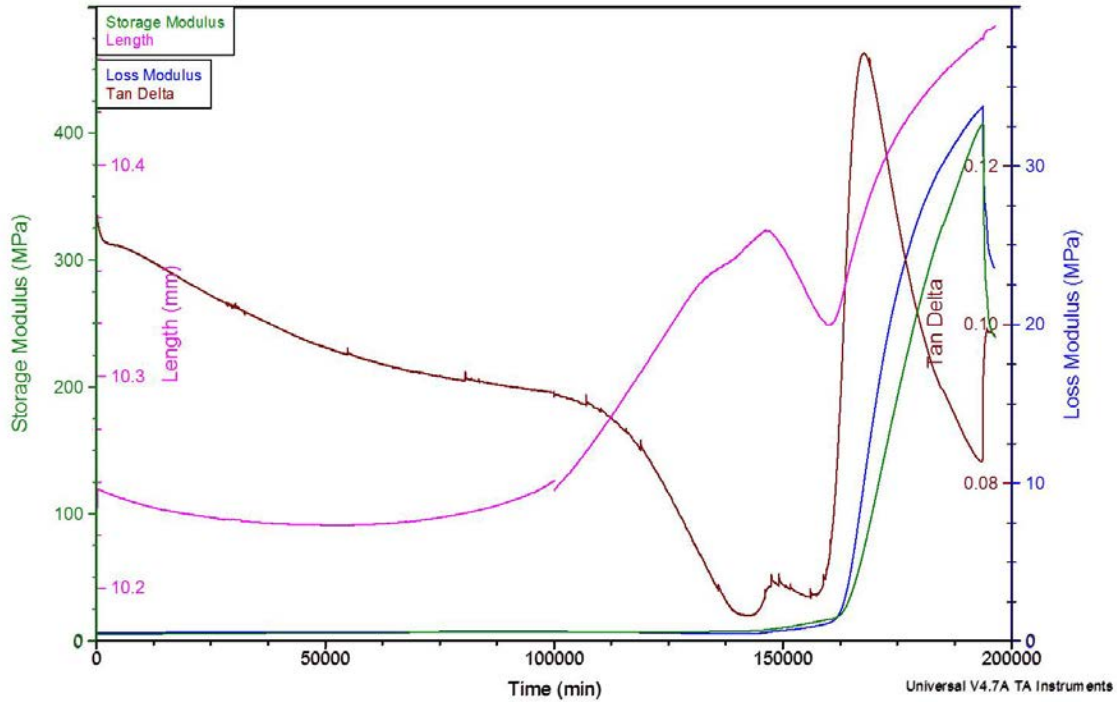


Figure 4.3. DMA Plot after 139 Days at 130°C in Air

4.2 Infrared Spectroscopy

As described in Section 3.3, ECQCL reflectance data over a narrow portion of the IR spectrum was obtained, to determine the benefits of a high-resolution reflectance measurement and the factors that may impact the sensitivity of the measurement.

The energies associated with infrared wavelengths of light correspond to the stretching and bending transitions in chemical bonds. FTIR can be a very sensitive method for identifying the presence of specific bonding in materials, such as carbon to oxygen double bonds (C=O, carbonyls), through characteristic infrared absorptions corresponding to those bonds. As chemical changes occur in cable insulation material with exposure to stresses including heat and radiation, the elimination of certain bonding and the creation of new bonds with chemical damage can be tracked with infrared spectroscopy.

Preliminary studies were conducted using the ECQCL using two specimens, one with no aging (Specimen 0), and one aged for 1200 hours (Specimen 13). The measurement setup for these studies was described in Section 3.3. It was decided that side-wall reflections were the most significant in terms of the end-use application, so the side-walls were interrogated first.

The raw data was normalized relative to a reference beam to achieve spectral reflectance. Reflectance can be calculated as:

$$R = P / P_0 \quad (4.1)$$

in which P_0 is the reference power spectrum from the ECQCL and P is the measured reflection from the side of the cable specimen. The reference spectrum was collected by reflecting the input beam off of a reflective copper surface. Reflectance is equal to unity minus transmission, absorption, and other losses. If we assume that absorption is the dominant mechanism of loss, then plotting the resulting data as in Figure 4.4 makes it easier to compare to FTIR transmission data than by looking at reflectance.

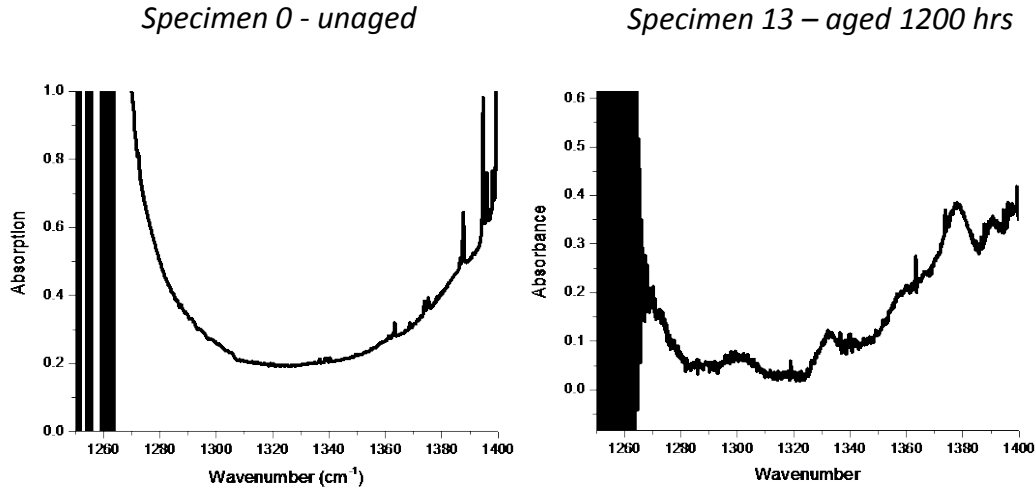


Figure 4.4. Side-wall Reflections from Specimens 0 and 13

Understanding what the results from Figure 4.4 mean is challenging because there are many possible sources of interference. First, the outside surface of the cables may be coated with an unknown residue, whether intentionally or unintentionally applied. The un-aged Specimen 0, in theory, should have shown a strong absorption peak around 1380 cm^{-1} , but in this scan it was not detected at all. In fact, this scan shows very little in the way of interesting features whatsoever.

Some aspects of these figures are intriguing, such as the appearance of a prominent absorbance peak around 1380 cm^{-1} in the aged specimen. On the other hand, the FTIR transmittance results seem to indicate that this same peak disappears when EPR is aged. These inconsistencies may require data on additional specimens to rule out other variables and confirm the effects observed in these measurements.

4.3 Indenter Measurements

Indenter modulus measurements were performed at PNNL using an Ogden Indenter Polymer Aging Monitor generously loaned by the Electric Power Research Institute. Segments of shielded and unshielded cables with EPR insulation were aged in 140°C ovens in air for up to 1200 hours. The indenter moduli measured at various time points for these two cable series are plotted in Figures 4.5 and 4.6. In the case of the cable with no shielding or jacket, the measurement interrogates the EPR insulation directly. In the case of the shielded and jacketed cable, the measurement identifies changes in the PVC (polyvinyl chloride) jacket.

As the figures show, changes in indenter modulus are generally increasing with age in both cases, although the data from the unshielded cable show greater scatter. The increased scatter could be from non-uniform aging of the cables, although other factors such as experimental error cannot be ruled out at this stage. In any case, these data are likely indicative of the variability that may be expected from indenter measurements in the field.

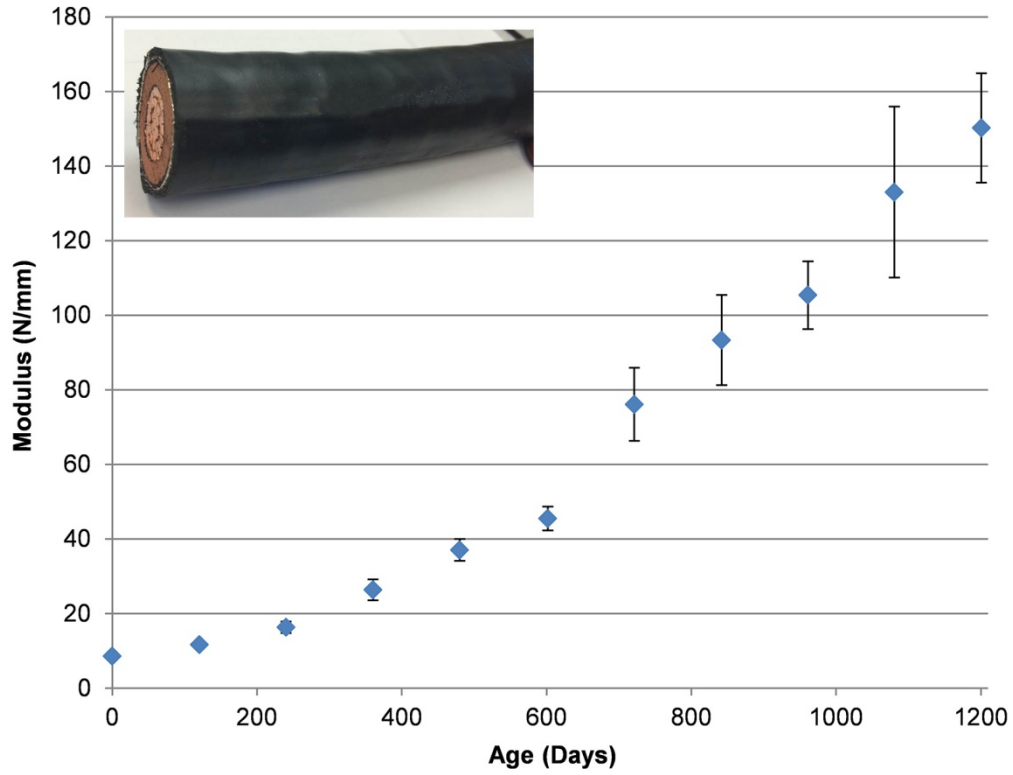


Figure 4.5. Plot of Indenter Modulus vs. Time at 140°C in Air for Shielded EPR Cables with Jacket

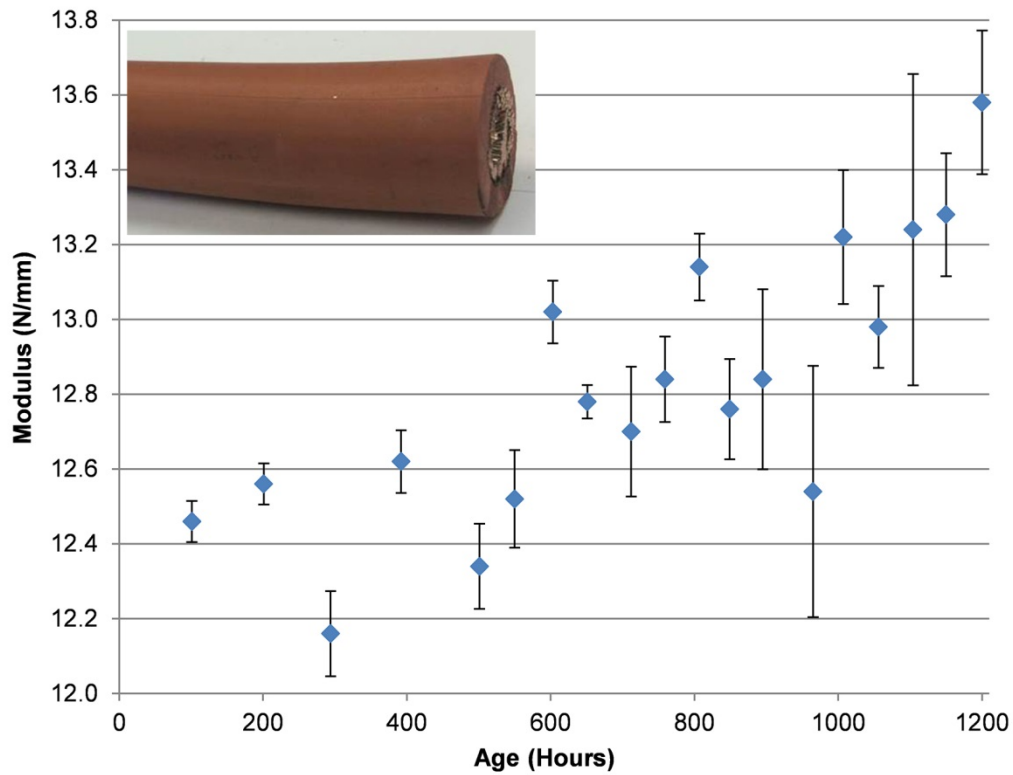


Figure 4.6. Plot of Indenter Modulus vs. Time at 140°C in Air for Unshielded EPR Cables without a Jacket

4.4 Acoustic Measurements

For this study, a total of nine cable segments (C2-C10 in Table 4.1) with EPR insulation were used for testing. The specimens (see Figure 4.7) are 12.7 cm (5 in.) in length, and 2.54 cm (1 in.) in total diameter. The insulation thickness is approximately 0.5 cm (0.2 in.), and the segments were aged at 140°C. The time each specimen was aged varied from 101 hours to 1056 hours, as shown in Table 4.1. Two different arrangements of probes were used to measure the ultrasonic surface wave and compute the sound speed. The measurement protocol for each of these arrangements, along with the results, is described next.

Table 4.1. Summary of Cable Specimens and Aging Condition Used for Acoustic Measurements

Specimen ID	Hours
C2	101
C3	201
C4	392
C5	603
C6	849
C7	895
C8	965
C9	1007
C10	1056

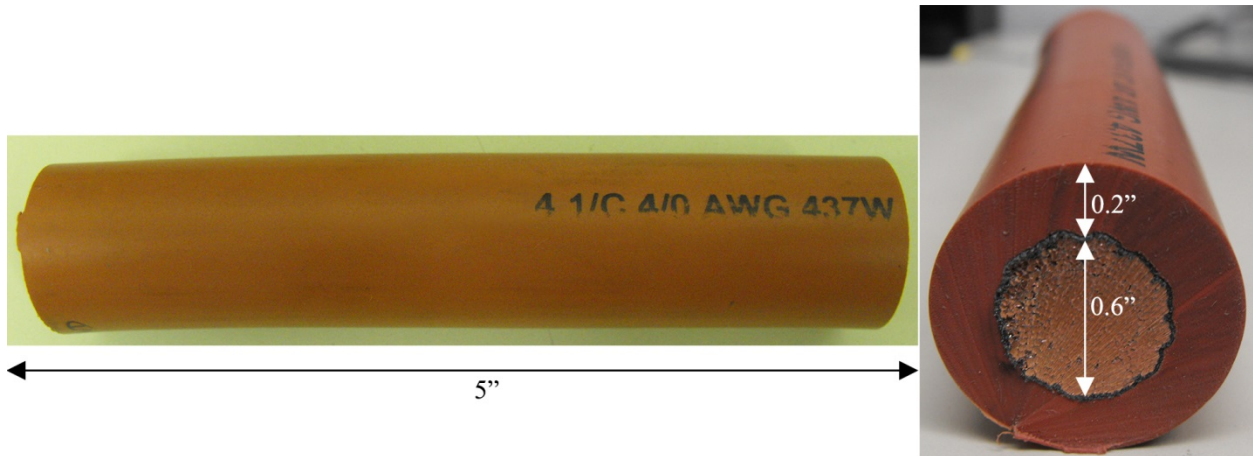


Figure 4.7. Top View (left) and Side View (right) of the Cable Specimen Used in the Guided Wave Inspection for Thermal Aging

4.4.1 Conventional Transducer Measurements

Two conventional ultrasound piezoelectric transducers with 2.54-cm (1-in.) diameter and 150-kHz center frequency are used in a pitch-catch configuration. The experimental setup is shown in Figure 4.8. A function generator is used to directly excite the transmitting transducer with a 20 V peak-to-peak 4-cycle Hanning windowed toned burst with 150-kHz center frequency. The receiving transducer is connected to a preamplifier with a fixed gain of 40 dB, and the output of the preamplifier is connected to an oscilloscope. Standoffs were fabricated so that the transducers could be mounted on top of the cable with the transducer surface directly touching the cable, as shown in Figure 4.9.

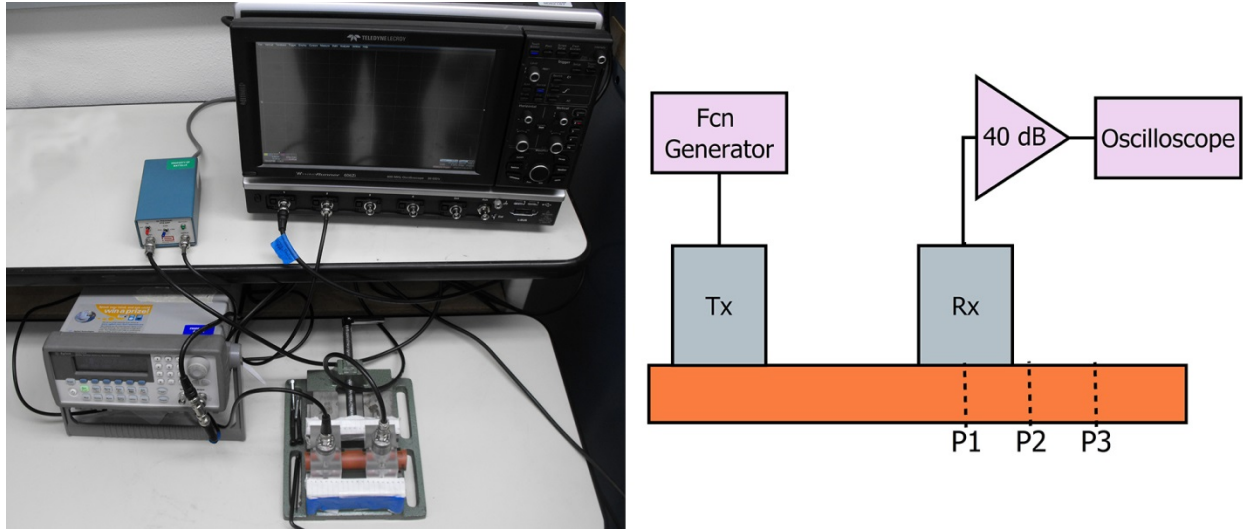


Figure 4.8. Experimental Measurement Setup (left), and a Block Diagram Representing the Setup (right). The three measurement points collected on each cable are shown as P1, P2, and P3.

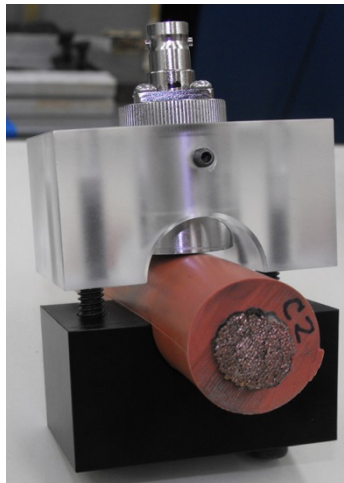


Figure 4.9. 2.54-cm (1-in.) Diameter Transducer Mounted on Top of an EPR Rubber Cable

Collected data is saved using an oscilloscope for subsequent post-processing. Three measurement points are collected on each of the nine cable specimens. The transmitting transducer is fixed near the edge of the cable (see Figure 4.8), and the receiving transducer is positioned approximately 9 cm (3.5 in.) from the transmitter. Then the receiving transducer is moved by 1 cm (0.4 in.) away from the transmitter, data recorded, and the process repeated. The exact distance was measured using a Vernier caliper. The time series measurements obtained from cable C2 and C10 are shown in Figure 4.10. This data is used to extract the time of flight of the wave field.

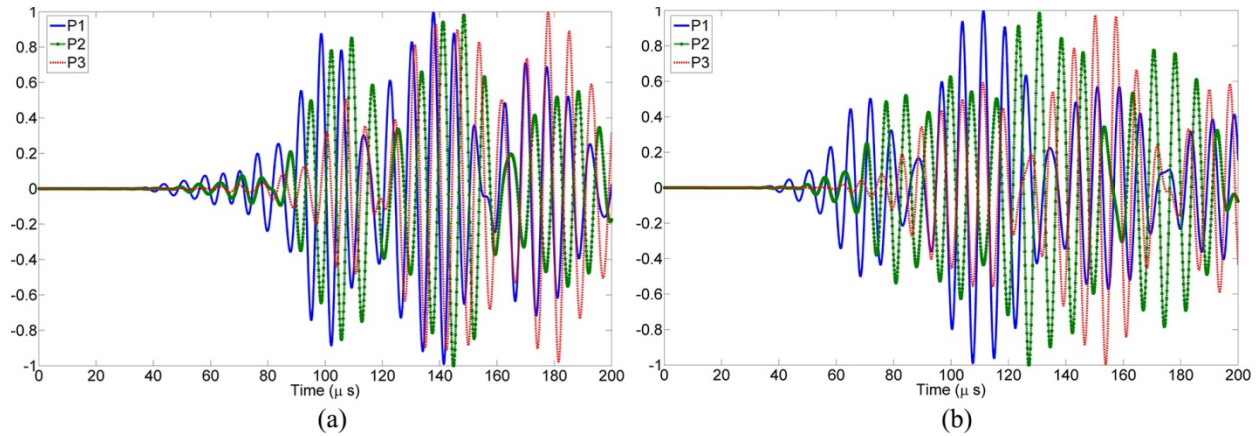


Figure 4.10. Time Series Measurements with the Three Measurement Points for (a) Cable C2 and (b) Cable C10

Because of the complicated nature of the waveforms, a time-frequency analysis was conducted. The short-time Fourier transform (STFT) was computed from the time domain signals (Figure 4.11(a) presents an example spectrogram obtained from measurements on cable specimen C2). The window size used in the STFT is $1/2B$, where B is the bandwidth of the 4-cycle Hanning window tone-burst excitation signal (150 kHz). Then, the component of the spectrogram at the excitation center frequency of 150 kHz is extracted to obtain the time domain signal at that specific frequency (Figure 4.11(b)). The first wave packet time of flight is estimated by computing the time at which the signal amplitude goes above -60 dB in amplitude relative to the peak amplitude. Then, the wave speed velocity is computed using the measured distances between the consecutive receiver measurement positions. A total of three wave velocity estimates were obtained for each cable specimen. The resulting computed velocity as a function of thermal aging time is shown in Figure 4.12. As seen from the data, the results do not appear to show any specific trend of the wave speed with increasing age, and there is significant variability in the computed wave speed for each cable specimen. However, this does not necessarily indicate that there is no correlation between wave speed and thermal aging. It appears that the measurements obtained are inconsistent because of the following factors:

- The waveform shape changes between consecutive measurements on the same cable specimen. This is because the receiver transducer and its standoff need to be moved manually, which might result in different bending on the cable (boundary conditions), which affects the signal shape.
- The way that the time of flight is measured is affected by the noise level in the signal, which does not allow perfect estimation of the time of arrival of the first wave packet. Also, interfering wave packets because of reflections from edges make it difficult to find a unique wave peak that could be used to infer the time of flight.

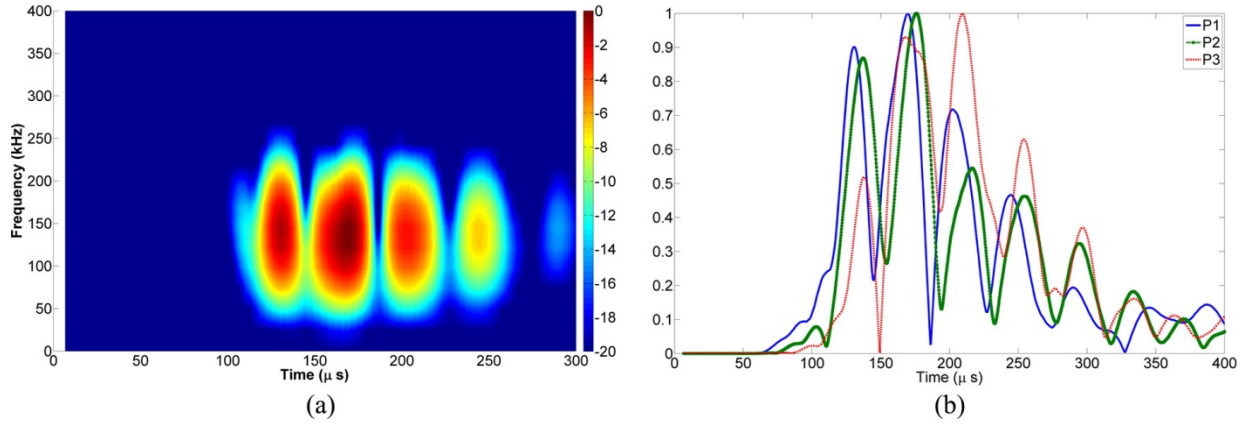


Figure 4.11. (a) Spectrogram of the Measurement Obtained at P1 on Cable Specimen C2. (b) The Spectrogram Plotted at the Excitation Center Frequency of 150 kHz for the 3-Position Measurement on Cable Specimen C2.

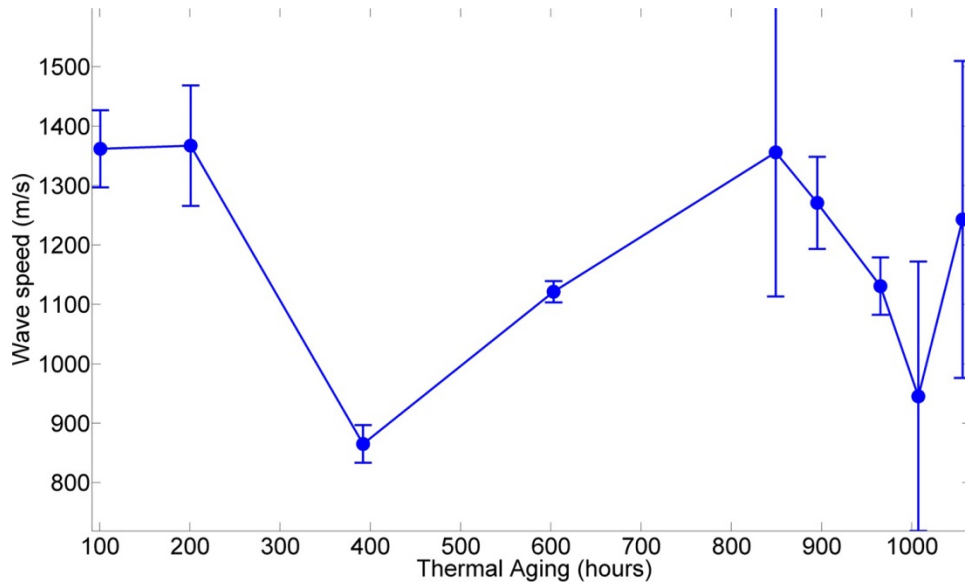


Figure 4.12. Wave Velocity Estimation for All the Nine Cable Specimens with Different Thermal Aging Times

4.4.2 Scanning Pinducer Measurements

Because of the difficulties encountered with the conventional transducer approach, another method was considered that allows obtaining more information about the propagating wave field in the EPR rubber cable. A 150-kHz transducer with 1.9-cm (0.75-in.) diameter (Physical Acoustics R15a) was used for excitation by placing it directly on the cable surface. The transducer was connected to a function generator and excited with a 5-cycle 150-kHz Hanning windowed tone burst. A Valpey-Fisher 1-mm (0.04-in.) diameter pinducer is mounted on a step motor and coupled to the surface of the cable by immersing it into water, as depicted in Figure 4.13. The pinducer is scanned axially on the cable surface with 0.5-mm (0.02-in.) steps for a total of 20-mm (0.8-in.) distance. Three cables (C2, C4, and C13 in Table 4.1) with different thermal aging were scanned using this approach to assess feasibility.

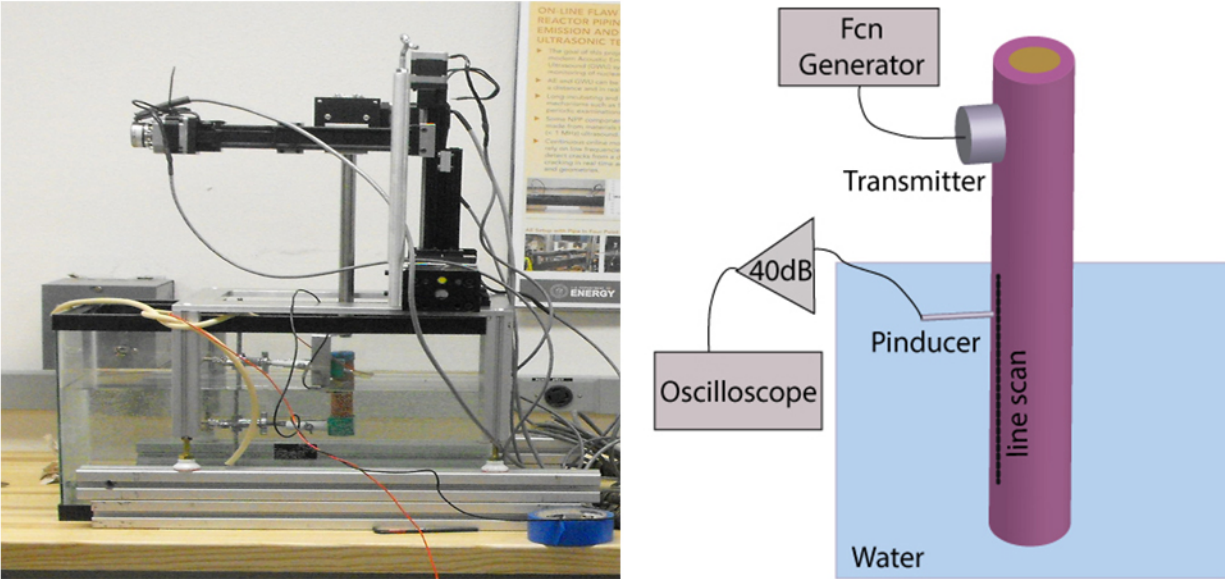


Figure 4.13. Experimental Setup for Scanning the Pinducer Along the Surface of the Cable

The scan data gives an image showing the wavefront propagation along the scanned line, as shown in Figure 4.14. Note that as time increases, some of the wavefronts seem to be propagating back, and this is because of the superposition of both forward propagating waves, and reflections from the cable edges propagating backward. The first arriving wavefront does not have interferences from back-propagating waves and its slope gives the surface-wave velocity. The procedure to compute the wave velocity from the wave front image is as follows:

1. The wavefront arrival time at position 0 was recorded from the image. The time between the zero crossings of this wavefront were extracted. Then, an iterative procedure was used to compute the zero crossings at the remaining scan positions. The extracted wavefront is shown in Figure 4.15.
2. A least square linear polynomial: $c_1t + c_2$, where t is time, was fitted to the extracted waveform, shown in Figure 4.15.
3. The slope of the fitted line and the surface wave speed is c_1 .

This procedure is performed for the three first arriving wavefronts for each of the three cables. The computed wave speed results are shown in Figure 4.16. The wave speed in the cable with 1200 hours of thermal aging is about 70 m/s less than the other two cables with 101 hours and 392 hours of thermal aging.

While this specific arrangement is unlikely to be applicable in-situ, it provides an indication that measurable changes in sound speed are possible with thermal aging. The challenge at this stage is identifying the cause of the apparent reduction in sound speed with age. A lowered sound speed, especially in viscoelastic materials, indicates an increase in density and/or a reduction in the elastic modulus. The DMA data (Section 4.1), however, indicate an increase in the storage and loss moduli with age for these same materials, when aged under similar conditions. If so, increases in density may be the driving factor for the reduction in sound speed. This is hypothetical at this stage and requires a measurement of the density of these materials as well as confirmation of the decreasing trend using additional specimens; these measurements are ongoing.

Note also that the probe arrangement shown (with the cable segment partially submerged in water, and water used as a couplant medium) is not likely to be useful in an in-situ setting. However, the setup may be modified for field use through the addition of multiple pinducers (microprobes) that gather measurements as a function of distance from the transmitting probe. In this respect, this arrangement is merely a finer resolution version of the conventional transducer arrangement described in Section 4.4.1. When applied in-situ, the measurements are unlikely to be contaminated with spurious reflections from the ends of the cable segment as was the case in Section 4.4.1.

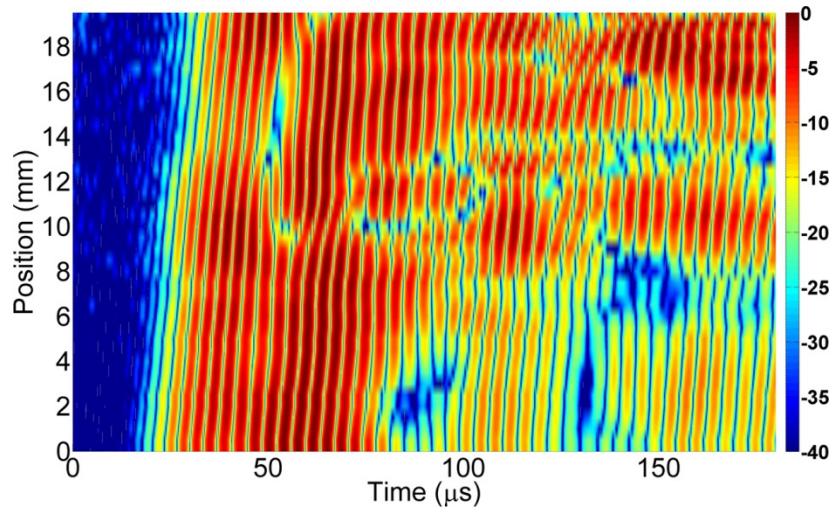


Figure 4.14. Wavefront's Shape as they Propagate in Time, Obtained from the Scan Measurements

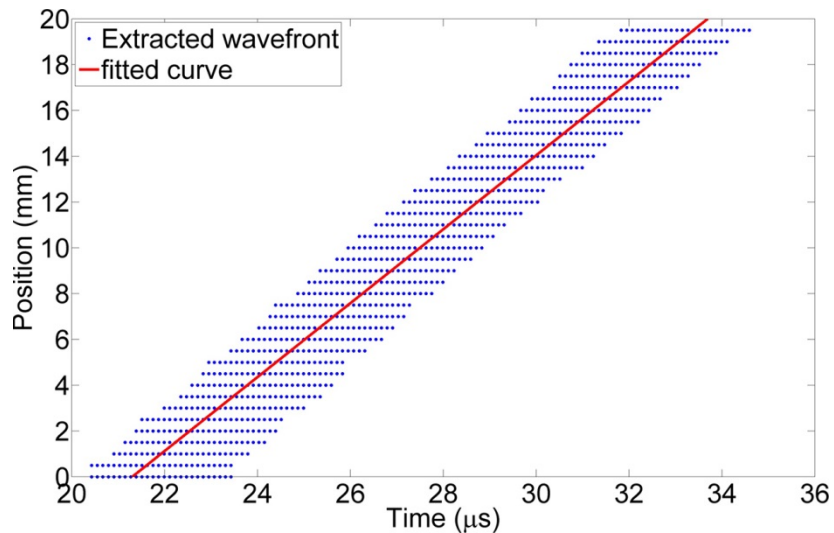


Figure 4.15. A Single Wavefront Extracted from the Image, and Its Linear Fit

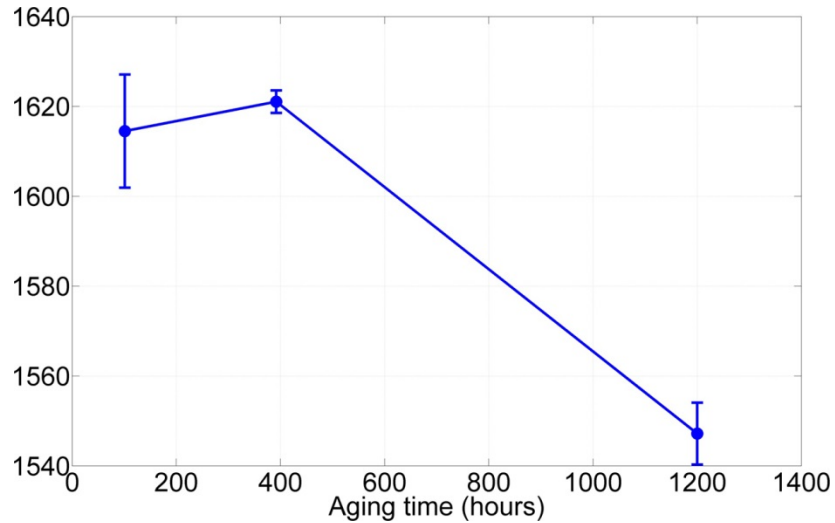


Figure 4.16. Computed Wave Speed for the Three Cable Sections with Different Thermal Aging Times

4.5 Coaxial Dielectric Probe Measurements

Recent complex permittivity measurement results from the dielectric probe studies demonstrated trends in an increase of the real part of the dielectric constant vs. sample age. Challenges presented with the high-temperature probe method include maintaining repeatable pressure, preserving clean calibration as the VNA thermally drifts on a very small level but still significant to the accuracy of our data.

The most recent data results are shown for small cable square samples (Figure 4.17) that are ideal for mechanical stress tests but electrically thin for the dielectric measurements. This will provide a means for comparing mechanical testing to dielectric properties. There were a total of 63 physical samples, representing 21 unique time stamps. Each physical sample was measured four times in order to remove measurement drift and incoherent noise effects from the measurement.

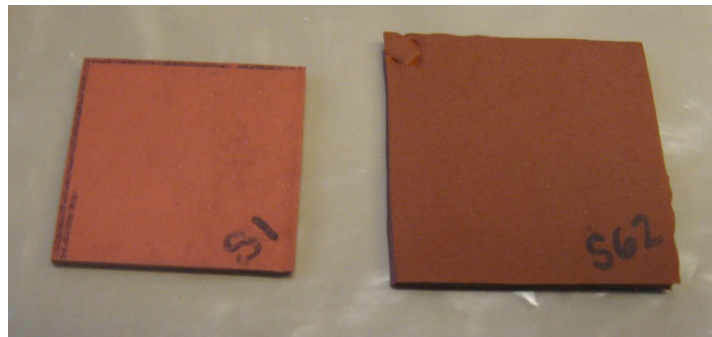


Figure 4.17. Cable Housing Square Samples

The raw data is originally collected as the dielectric constant vs. frequency. It was observed that there is a small amount of higher-frequency noise riding on the dielectric constant data; therefore, a low-pass filter was applied to the data in MATLAB™ improving our sensitivity and reducing outlier data points. In order to more readily identify trends, viewing the data in terms of real part of the dielectric constant vs. exposure time for single frequency samples proved to be more advantageous. The low-pass-filtered 252 data points are shown in Figure 4.18.

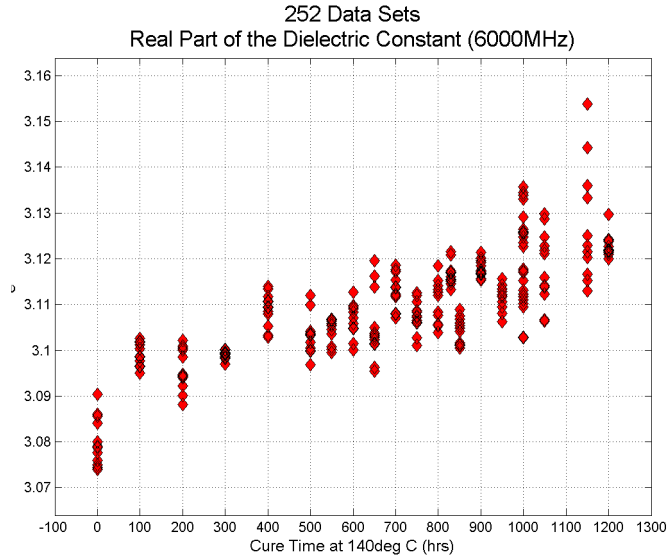


Figure 4.18. Real Part of the Dielectric Constant for All Samples at 6000 MHz vs. Cure Time at 140°C

Next, the four measurements for the real dielectric constant for each physical sample were averaged and plotted vs. exposure time to 140°C shown in Figure 4.19.

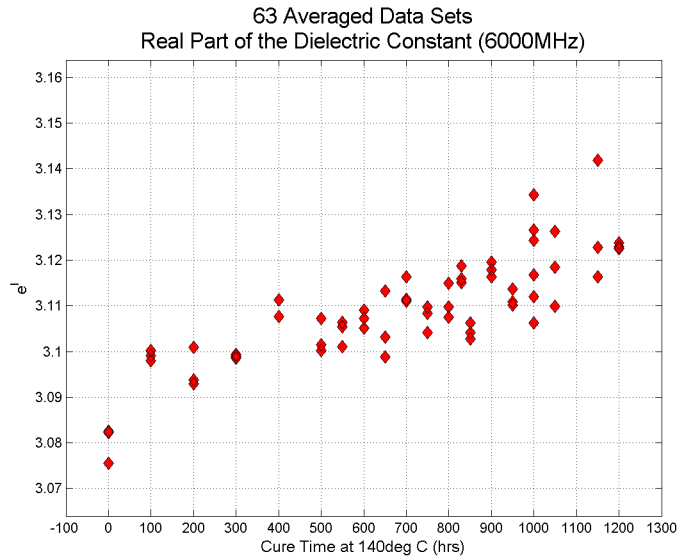


Figure 4.19. Averaged Real Part of the Dielectric Constant at 6000 MHz vs. Cure Time at 140°C for Each Physical Sample

Once the data were averaged, the mean was calculated for each time stamp (Figure 4.20). The standard deviation was also plotted as an error bar. In some cases, the error bar is quite large, but one can observe the trend even in these electrically thin cable housing samples.

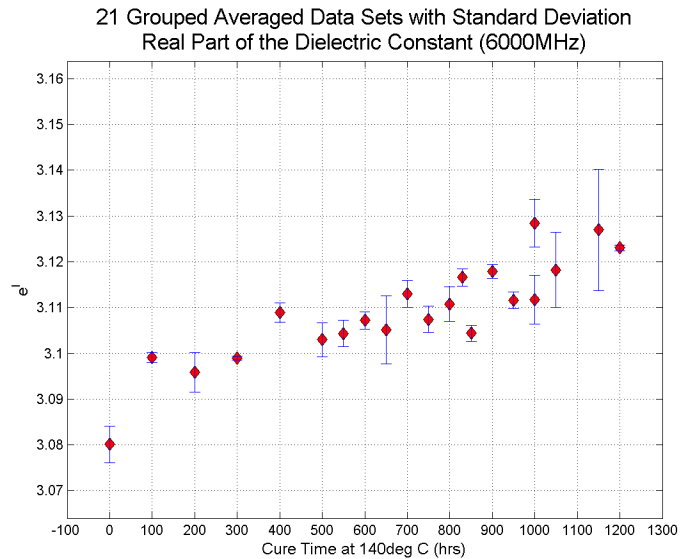


Figure 4.20. Mean Value of Real Part of the Dielectric Constant with Standard Deviation at 6000 MHz

4.6 Discussion

Several approaches to measuring key indicators of cable aging and degradation are available, and include chemical, mechanical, and electrical measurements. Measurements to date (electrical, mechanical) reinforce the assessment that measurements of dielectric permittivity (as measured using the coaxial dielectric probe (related to $\tan \delta$)) and sound speed (using a scanning microprobe) are capable of providing information on cable age (and potentially remaining useful life). However, the measurements also indicate a certain level of sensitivity to a number of other factors, including the fixture used for the probe as well as physical effects (surface damage) of the accelerated aging methodology.

ECQCL reflection spectra may be capable of sensitively tracking chemical changes in materials with thermal oxidation stress. Carbonyl chemical groups that form by reaction of thermally induced radicals in the material with oxygen present have characteristic absorption peaks. The presence and extent of these peaks is a key indicator of cable aging. Because absolute peak intensity can vary with specimen geometry, it may be useful to determine internal references in the spectra. Ratios between peaks that change with aging and those that do not can then be used a metric of aging comparable between different cables. However, data to date were inconclusive, and may have been influenced by surface conditions that form due to the accelerated aging process in EPR materials.

The DMA has been determined to be a valuable tool for monitoring property changes over time. However, it is unlikely to be directly applicable in an in-plant setting; instead, it provides valuable insights into the mechanical property changes of polymers with thermal aging. These insights may be applied to the development of alternate in-situ mechanical measurement methods (such as acoustic measurement methods).

Data from aged EPR sheets confirm the applicability of dielectric measurements to track the level of aging. Uncertainties inherent in the measurement (particularly due to insufficient material thickness for optimal use of the dielectric probe described in Section 3.5.1.1) will need to be addressed if such measurements are to be made in-situ in nuclear plants. However, the changes in dielectric properties with age will likely contribute to measureable changes from reflectometry measurement methods (such as time-domain reflectometry, frequency domain reflectometry, and line-resonance analysis). These NDE measurement techniques will be evaluated further going forward.

In contrast, the acoustic measurement methods need further study to confirm that sound speed (and potentially attenuation) may be an indicator of age that directly correlates with indenter modulus and EAB, and to design protocols that translate the laboratory-scale approach to an in-situ measurement approach. Additional studies may also be needed to determine the viability of approaches that directly measure changes in polymer chemistry as a result of aging; these are planned for future phases of research.

5. SUMMARY

The aging of cables is considered to be one of the factors that may limit the ability of light water reactors to continue operations beyond their licensed period (up to 60 years, depending on the specific plant). The most important requirement for cables (electrical or instrumentation) in NPPs is the ability to withstand a design-basis accident. Aging and subsequent degradation of insulation will impair the ability of cables to perform their function under all conditions, and there is therefore a need to assess the condition of cable insulation and estimate the corresponding remaining useful qualified life of the cable.

Several approaches to nondestructively measuring key indicators of cable aging and degradation are available and include chemical, mechanical, and electrical measurements. Electrical and acoustic measurements are potential NDE approaches that may be capable of providing in-situ assessments of cable condition and remaining useful life.

This report is the latest in a series of reports, each documenting studies on a subset of key indicators. The present document reported on the ability to measure mechanical moduli using stress-wave-based interrogation methods, as well as the feasibility of applying higher resolution IR reflectance spectroscopy. Supporting laboratory-based measurement methods that provide insights into the changes in material properties with thermal aging are also presented.

In each case, measurement studies were conducted with specimens of aged medium-voltage EPR cable. Accelerated aging studies were conducted at multiple temperatures using the cable system (short segments of cable with the conductor intact). A test-bed was also fabricated to enable in-situ measurement of current and voltage on an aging cable system (conductor and insulation), along with aging of the smaller specimens of the medium-voltage cable. These specimens were used for measurements of key indicators.

Previous studies with EPR indicated that the complex electrical permittivity appeared to show correlation with aging while preliminary studies on acoustic sound speed showed no clear measurable trend (within the error bounds). The primary factor impacting the measurements in the previous study was the unknown and variable thickness of the insulating material. In this study, the measurement protocols were modified to overcome this issue, and to use higher precision probes within a laboratory-scale measurement setup. Measurements of acoustic wave speed using this modified setup show a measurable trend with aging, although the results are based on a small set of specimens. Further, in-situ measurements using dynamic mechanical analysis indicate that the storage modulus changes with specimen age; this change is a function of the aging conditions and the environment the specimen is in. However, laboratory-scale measurements using higher resolution IR reflectance spectroscopy (albeit over a narrow portion of the IR spectrum) were inconclusive. It is likely that this result is due to unknown surface conditions on the aged specimens.

Additional studies are ongoing to determine the viability of these approaches for other insulating materials (such as XLPE) that are common in NPPs.

All of the measurements obtained to date were on EPR specimens. Additional measurements on EPR specimens aged at different temperatures (100°C and 124°C) are ongoing, although the completion of this activity is awaiting the completion of accelerated aging of specimens at these temperatures. Similarly, accelerated aging of XLPE specimens is ongoing, with measurements keeping pace as specimens are extracted periodically. Data from these specimens, as well as the use of these key indicators in advancing the state of the art in NDE methods, is ongoing.

The accelerated aging of specimens at several different temperatures is being conducted in parallel, enabling the building of a library of specimens with different materials and differing aging conditions. At the same time, we are looking to leverage specimens from ongoing studies on joint thermal/radiation aging that are being conducted in a companion project. We are also looking to leverage measurement techniques from collaborations formed under a NEUP project. Results of these ongoing studies will be presented in upcoming technical reports. Finally, focus is shifting to develop in-situ measurement approaches for key indicators that show promise, and to evaluate such advanced NDE techniques for sensitivity and reliability.

6. PATH FORWARD

Research going forward will focus on completing accelerated thermal aging of EPR and XLPE at multiple temperatures, the viability assessment of measurements of chemical, mechanical, and electrical key indicators on these specimens correlated to cable aging, and determine whether these diverse sets of measurements can provide synergistic information that can more effectively help in decisions on repair and replacement. Analysis of the viability will also require assessment of deployment challenges for the measurement methods employed for each of the key indicators. While most of the mechanical and electrical key indicator measurements may be performed on the complete cable system, issues such as variable thickness of the insulation, or the presence of shielding, may challenge the sensitivity of the measurement. Such issues will also be evaluated going forward.

Going forward, the following measurement methods are expected to be developed further with an eye towards feasible implementation in the field.

6.1 Mechanical Measurements

6.1.1 Ultrasonic Testing

Both the longitudinal-wave-speed and the surface-wave-speed methods will be investigated further, using EPR and XLPE materials. For the longitudinal-wave-speed method, a dual-mode system is under consideration, which allows both accurate measurement of the cable insulation thickness and longitudinal-wave measurement. An eddy-current electromagnetic technique is being investigated for measuring the insulation thickness.

For the surface-wave method, additional investigation of the wave nature is underway. First, the interactions between multiple wave modes that might be excited in the rubber insulation using the normal beam transducers will be studied. Second, rubbers are highly viscoelastic material, which introduces dispersive behavior in waves and the wave speed becomes a function of frequency. The change of viscoelastic behavior of the rubber insulation with aging needs to be well understood to be able to select proper transducers and operating frequency for wave measurements. Third, the effect of the interface between the rubber insulation and the conductor on wave propagation should be studied.

6.1.2 Alternative Measurements

As the study progresses, additional mechanical measurement techniques will be evaluated. These evaluations can be directly correlated to existing relevant data acquired by the indenter-type nondestructive tests as well as the EAB data that have been evaluated both in the laboratory and in the field on existing power plants.

- **DMA** – Future work with the DMA will be to continue to run isothermal runs at different temperatures and monitor the changes materials. The time-temperature-superposition method will be evaluated in predicting material changes relative to over time at different operating temperatures. The DMA modulus data will be used to assist the ultrasonic testing methods in determining the effects on bulk velocity and surface-wave measurements.
- **Non-linear Ultrasonic Testing** – Ongoing efforts in measuring the non-linear ultrasonic coefficient for cable insulation are focusing on using measurement protocols that are commonly applied to metals. The approach described previously, based on measurements conducted in medical ultrasonics, is useful in a laboratory setting. Although this exact water-tank approach typically requires larger specimen sizes than are commonly available with insulators and is not practical for in-situ measurement a modified, a modified approach that will at least generate a measurable signal that will be proportional to the absolute B/A parameter is planned for further evaluation.

6.2 Electrical Measurements

As the study progresses, additional electrical measurement methods will be investigated. These methods will be assessed on the test apparatus and evaluated as possible methods for further exploration. Some of the methods currently being considered are:

Electrical Permittivity – The electrical permittivity measurements (using the coaxial probe and capacitance probe) that were initially investigated will be further explored using additional specimens (EPR and XLPE, thermally aged and joint thermal/radiation aged).

Line Resonance Analysis – Line resonance analysis (LIRA) is a frequency-domain electrical reflectometry measurement technique that has been shown to detect changes in electrical impedance along a cable from a measurement made by connecting to one end of a de-energized cable. These changes are generally from changes in the dielectric properties of the insulation material or to irregularities in the wire geometry. LIRA has been used to assess damage along AC and DC signal and power cables for various industries such as oil and gas, power transmission and distribution, offshore wind, and nuclear power (<http://wirescan.no/references>). Example changes that impact the insulation capacitance include cable joints and splices as well as locations that have been subject to heat, radiation, water damage, corrosion, or mechanical fatigue. A commercially available system for line resonance analysis is shown in Figure 6.1. The system injects a low-voltage signal into the cable via a probe connection to two conductors. The measurement process takes approximately 1–2 minutes and the data can be stored for offline post-processing. Challenges in applying the technique to the nuclear power industry include prediction of remaining life, characterizing energized cables for continuous condition monitoring, and measuring unshielded single conductor cables in isolation.



Figure 6.1. LIRA Portable System for Assessing the Condition of Electrical Cables

The technique is based on transmission line theory and is valid when the cable length is at least comparable to the wavelength of the electromagnetic signals propagated along the cable. Commercially available systems have an upper frequency limit and consequently have minimum cable lengths below which measurement reliability may suffer. Available data typically consists of a complex impedance spectrum for a user-defined frequency range; this data is used to calculate cable parameters and signatures, which can indicate both local and global degradations. Figure 6.2 shows an example complex impedance spectrum for a cable measurement using a frequency bandwidth of 50 MHz. The maximum cable length that can be examined using this technique is dependent on the attenuation of the signal as it propagates to and from the instrument.

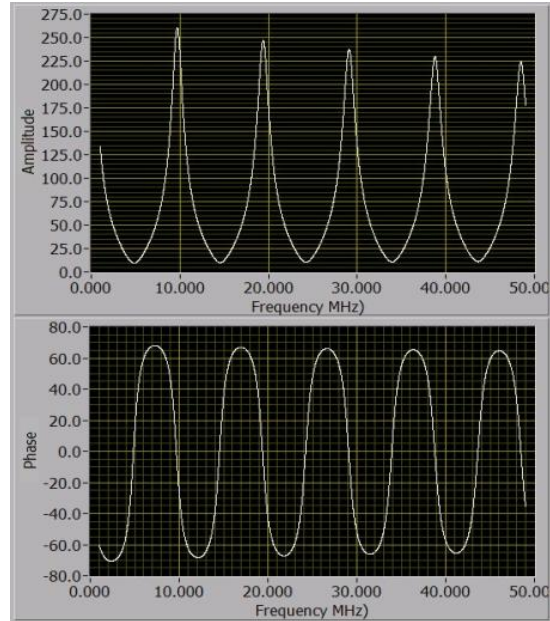


Figure 6.2. An Example Impedance Spectrum which Forms the Basis for All Cable Evaluations Performed by Line Resonance Analysis

Simulator modules may be used to perform parametric or “what-if” studies for cable degradation scenarios. The results from the simulator can be analyzed by the system as if they were obtained from a real measurement. This allows the operator to compare measured and predicted results for a given cable under test.

We plan to use commercially available instruments to investigate the sensitivity of extracted cable signatures to changes in the cable input parameters such as line capacitance and insulation dielectric constant, and determine if these measurements are a potential replacement for other cable condition indicators such as EAB and indenter modulus. Previous work has indicated that local changes of approximately 10 pF/m in the line capacitance or 0.2 μ H/m in the line inductance can be reliably detected (Fantoni and Nordlund 2006).

7. REFERENCES

- Appajaiah A, H-J Kretzschmar and W Daum. 2007. "Aging Behavior of Polymer Optical Fibers: Degradation Characterization by FTIR." *Journal of Applied Polymer Science* 103(2):860-870.
- Bowler N and S Liu. 2015. "Aging Mechanisms and Monitoring of Cable Polymers." *International Journal of Prognostics and Health Management*. Submitted February 2015.
- Curl RF, F Capasso, C Gmachl, AA Kosterev, B McManus, R Lewicki, M Pusharsky, G Wysocki and FK Tittel. 2010. "Quantum Cascade Lasers in Chemical Physics." *Chemical Physics Letters* 487(1-3):1-18.
- Ensminger D and LJ Bond. 2011. *Ultrasonics: Fundamentals, Technology and Applications, Third Edition (Revised and Expanded)*. CRC Press, Boca Raton, Florida.
- EPRI. 1994. *Low-Voltage Environmentally-Qualified Cable License Renewal Industry Report; Revision 1*. TR-103841, Electric Power Research Institute (EPRI), Palo Alto, California.
- EPRI. 2005. *Initial Acceptance Criteria Concepts and Data for Assessing Longevity of Low-Voltage Cable Insulations and Jackets*. TR-1008211, Electric Power Research Institute (EPRI), Palo Alto, California.
- Fantoni PF and A Nordlund. 2006. *Wire System Aging Assessment and Condition Monitoring (WASCO)*. NKS-130, Nordic Nuclear Safety Research, Roskilde, Denmark.
- Gillen KT, M Celina and RL Clough. 1999. "Density Measurements as a Condition Monitoring Approach for Following the Aging of Nuclear Power Plant Cable Materials." *Radiation Physics and Chemistry* 56(4):429-447.
- IAEA. 2000. *Assessment and Management of Ageing of Major Nuclear Power Plant Components Important to Safety: In-containment Instrumentation and Control Cables. Volume I*. IAEA-TECDOC-1188, International Atomic Energy Agency, Vienna, Austria.
- IAEA. 2012. *Assessing and Managing Cable Ageing in Nuclear Power Plants*. IAEA Nuclear Energy Series No. NP-T-3.6, International Atomic Energy Agency (IAEA), Vienna.
- IEC. 1996. *Determination of Long-Term Radiation Aging in Polymers - Part 2: Procedure for Predicting Aging at Low Dose Rates*. IEC1244-2, International Electrotechnical Commission (IEC).
- IEC/IEEE. 2011. *International Standard: Nuclear Power Plants - Instrumentation and Control Important to Safety - Electrical Equipment Condition Monitoring Methods - Part 2: Indenter Modulus*. IEC/IEEE 62582-2, International Electrotechnical Commission (IEC), Geneva Switzerland; and Institute of Electrical and Electronics Engineers, Inc., (IEEE), New York, New York.
- Ikehara J, T Ikeda, T Ashida and M Fujii. 1998. "Degradation Diagnosis of Polymeric Materials Using Ultrasonic Waves." In *Proceedings of the 1998 Ultrasonics Symposium*, pp. 1667-1170, Vol. 2. October 5-8, 1998, Sendai, Japan. DOI 10.1109/ULTSYM.1998.765046. Institute of Electrical and Electronics Engineers Inc., Piscataway, New Jersey.
- JNES. 2009. *Final Report of Assessment of Cable Aging for Nuclear Power Plants*. JNES-SS-0903, Japan Nuclear Energy Safety Organization (JNES), Tokyo.

- Krautkrämer J and H Krautkrämer. 1990. *Ultrasonic Testing of Materials, 4th Fully Revised Edition*. Springer-Verlag, New York. p. 69.
- Kusano J and Y Uno. 2003. *Radiation Resistivity of Polymeric Materials with Data Tables*. JAERI-Data/Code--2003-015, Japanese Atomic Energy Research Institute, Japan.
- Lee KI. 2013. "Correlations of Linear and Nonlinear Ultrasound Parameters with Density and Microarchitectural Parameters in Trabecular Bone." *The Journal of the Acoustical Society of America* 134(5):EL381-EL386.
- Lofaro R, E Grove, M Villaran, P Soo and F Hsu. 2001. *Assessment of Environmental Qualification Practices and Condition Monitoring Techniques for Low-Voltage Electric Cables: Condition Monitoring Test Results*. NUREG/CR-6704, Volume 2, U.S. Nuclear Regulatory Commission, Washington, D.C.
- Mailhot B, P-O Bussière, A Rivaton, S Morlat-Thérias and J-L Gardette. 2004. "Depth Profiling by AFM Nanoindentations and Micro-FTIR Spectroscopy for the Study of Polymer Ageing." *Macromolecular Rapid Communications* 25(2):436-440.
- Mantey A and G Toman. 2013. *Plant Engineering: Aging Management Program Guidance for Medium-Voltage Cable Systems for Nuclear Power Plants, Revision 1*. Technical Report 3002000557, Electric Power Research Institute, Charlotte, North Carolina.
- Menard KP. 2008. *Dynamic Mechanical Analysis: A Practical Introduction, Second Edition*. CRC Press, London.
- Namouchi F, H Smaoui, N Fourati, C Zerrouki, H Guerhazi and JJ Bonnet. 2009. "Investigation on Electrical Properties of Thermally Aged PMMA by Combined Use of FTIR and Impedance Spectroscopies." *Journal of Alloys and Compounds* 469(1-2):197-202.
- Nishida Y, K Itagaki, Y Yamaji, M Konishi, S Suzuki and T Yamamoto. 1999. "Non-destructive Diagnosis Technique for Aging of Cables Used at Nuclear Power Plants." In *ICONE-7: Proceedings of the 6th International Conference on Nuclear Engineering*. April 19-23, 1999, Tokyo. Japan Society of Mechanical Engineers. ICONE-7274.
- NRC. 2013. *Expanded Materials Degradation Assessment (EMDA), Volume 5: Aging of Cables and Cable Systems*. NUREG/CR-7153, Vol. 5; ORNL/TM-2013/532, U.S. Nuclear Regulatory Commission, Washington, D.C.
- Owens SE, ET Hauck and JL Rose. 2005. "A Novel Couplant Free Mediator Ultrasonic Rayleigh Wave Technique for Detecting Surface Cracks in Green Parts." In *SAE 2004 Transaction Journal of Materials and Manufacturing*, pp. 205-213. March 8-11, 2004, Detroit, Michigan. SEA International, Warrendale, Pennsylvania.
- Pao Y-H. 1983. "Elastic Waves in Solids." *Journal of Applied Mechanics* 50(4b):1152-1164.
- Phillips MC and BE Bernacki. 2012. "Hyperspectral Microscopy of Explosives Particles Using an External Cavity Quantum Cascade Laser." *Optical Engineering* 52(6):061302.
- Roberts RA. 1990. "Model of the Acoustic Microscope Response to Scattering by a Near-surface Void." *Journal of Nondestructive Evaluation* 9(2-3):181-196.

- Rose JL. 2004. *Ultrasonic Waves in Solid Media*. Cambridge University Press, Cambridge, United Kingdom.
- Seguchi T, K Tamura, T Ohshima, A Shimada and H Kudoh. 2011. "Degradation Mechanisms of Cable Insulation Materials During Radiation–thermal Ageing in Radiation Environment." *Radiation Physics and Chemistry* 80(2):268-273.
- Sepe M. 1998. *Dynamic Mechanical Analysis for Plastics Engineering (PDL Handbook Series)*. Plastics Design Library, Norwich, New York.
- Sheldon RT and N Bowler. 2013. "An Interdigital Capacitive Sensor for Quantitative Characterization of Wire Insulation." In *Review of Progress in Quantitative Nondestructive Evaluation, Vol. 32*, pp. 1578-1585. July 15-20, 2012, Denver, Colorado. American Institute of Physics, Mellville, New York.
- Simmons K, LS Fifield, MP Westman, JR Tedeschi, AM Jones, MS Prowant, AF Pardini and P Ramuhalli. 2014. *Determining Remaining Useful Life of Aging Cables in Nuclear Power Plants – Interim Study for FY2014*. PNNL-23624, Pacific Northwest National Laboratory, Richland, Washington.
- Simmons K, A Pardini, L Fifield, J Tedeschi, M Westman, A Jones and P Ramuhalli. 2013. *Determining Remaining Useful Life of Aging Cables in Nuclear Power Plants – Interim Study FY13*. PNNL-22812, Pacific Northwest National Laboratory, Richland, Washington.
- Simmons KL, P Ramuhalli, DL Brenchley and JB Coble. 2012. *Light Water Reactor Sustainability (LWRS) Program – Non-Destructive Evaluation (NDE) R&D Roadmap for Determining Remaining Useful Life of Aging Cables in Nuclear Power Plants*. PNNL-21731, Pacific Northwest National Laboratory, Richland, Washington.
- Suter J, B Bernacki and M Phillips. 2012. "Spectral and Angular Dependence of Mid-infrared Diffuse Scattering from Explosives Residues for Standoff Detection Using External Cavity Quantum Cascade Lasers." *Applied Physics B* 108(4):965-974.
- Theocaris PS and N Papadopoulou. 1978. "Propagation of Stress Waves in Viscoelastic Media." *Polymer* 19(2):215-219.
- Viktorov IA. 1967. *Rayleigh and Lamb Waves: Physical Theory and Applications*. Plenum Press, New York. ISBN 0306302861 9780306302862.
- Villaran M and R Lofaro. 2010. *Essential Elements of an Electric Cable Condition Monitoring Program*. NUREG/CR-7000; BNL-NUREG-90318-2009, U.S. Nuclear Regulatory Commission, Washington, D.C.
- Yamamoto T and T Minakawa. 2009. *The Final Report of The Project of 'Assessment of Cable Aging for Nuclear Power Plants'*. JNES-SS-0903, Incorporated Administrative Agency Japan Nuclear Energy Safety Organization, Nuclear Energy System Safety Division, Tokyo, Japan.